Report on the Scientific Validation of the chopped mode spectroscopy processing in the PHT pipeline

Phil Richards
(UK ISO Data Centre, CCLRC, RAL)

and

Ulrich Klaas
(ISOPHOT Data Centre at MPIA)

Version 1.0

September 9, 2002

Rutherford Appleton Laboratory, Chilton, UK

Contents

1 Introduction

This report follows a similar format to the scientific validation of OLP V10 [1]. The same calibration files were used, so the spectrophotometry is expected to be identical. This revalidation of the chopped PHT-S spectra assesses the improvements to the validation test cases arising from the introduction of the bi-weight averaging of the pair-wise differences into the data processing using the algorithm described in the next section.
The improvements in the quality of the spectra also resulted in changes being made to the handling of negative flux values in the processing and the generation of the SPD products. The test cases used for this revalidation of the chopped PHT-S spectra are identical to those used for the revalidation of OLP 10.

2 Caveat

Although there has been a significant reduction in the noise on the continuum spectra using the bi-weight mean deglitching, there are occasions where a single pixel is hit by a high energy particle which affects the responsivity of a pixel for a significant part of a measurement. This can result in spurious features in the spectrum if there are only a few on-off cycles in the measurement. An example can be found in the spectrum for Mrk231 where Fig 1 shows the long wavelength (SL) part of the spectrum (in Jy) plotted with the uncertainties. In this case, the apparent absorption feature in the spectrum at $\sim 10.55\mu$m, is only a $\sim 2\sigma$ event and, given the uncertainties, this feature is not significant. However, if there is a significant unidentified feature in a spectrum or the measured line ratios are not as expected, it is strongly recommended that the raw data for the pixels associated with the features are examined using PIA.
Also it should be noted that the effects of space weather have been observed to be more prominent in spectra taken towards the end of the science window in a revolution.

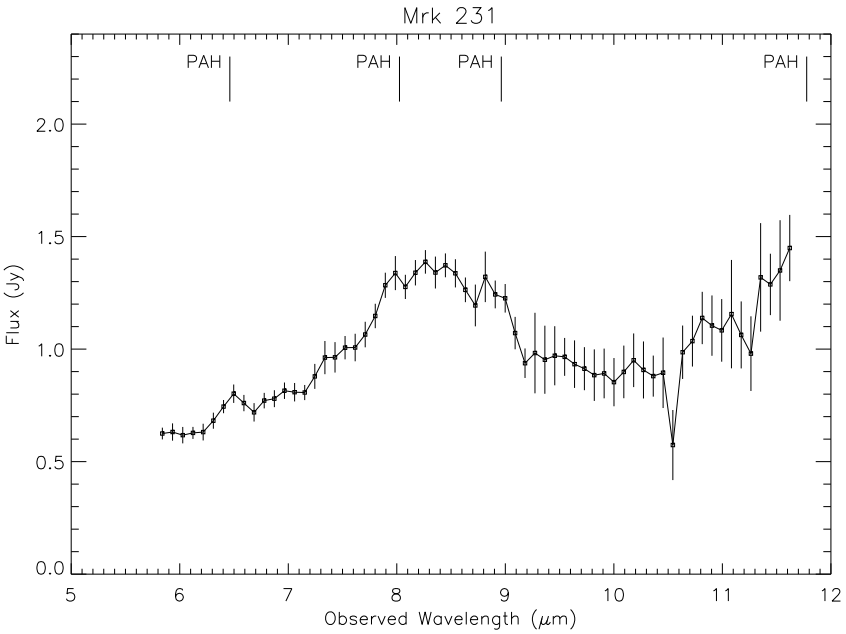

Figure 1: Spectrum for Mrk231 showing the spurious feature at $\sim 10.55\mu$m caused by a glitch from a high energy radiation hit.

3 The pipeline algorithm

In the PHT DERIVE_SPD, instead of processing the chopped measurement as a series of chopper plateaux using the ramp and signal processing described in sections 7.2 and 7.6.1

of the PHT Handbook [2], the average signal per chopper plateau has been derived from the difference signals from consecutive readouts.
The readouts used to determine the difference signals were filtered to remove:

- readouts that were saturated,
- readouts taken with the spacecraft off target.

All readouts on a ramp were used to derive difference signals, including those at the beginning of the ramp previously excluded from the ramp slope fitting and the destructive readout. However, the difference signal between the destructive readout and the first readout of the following ramp was excluded from the processing.
For all readouts accepted, the difference signal:

$$s_{diff} = \frac{V_{i+1} - V_i}{t_{i+1} - t_i}$$

where V_i and V_{i+1} are the CRE readout voltages (Volts) and t_i and t_{i+1} are the times (secs) of consecutive readouts. These difference signals are accumulated per pixel in arrays for the whole plateau.
When all difference signals have been accumulated, the mean signal for each pixel is derived by determining an outlier-resistant average using an implementation of the IDL procedure BIWEIGHT_MEAN from the Freudenreich AstroContrib Library. In addition to the mean, this routine returns the standard deviation of the distribution of difference signals from which the standard deviation of the mean is determined by dividing by the square root of the number of difference signals.
No corrections are applied to the bi-weight mean signals, so these signals and the weights from their standard deviations correspond to the s_k and w_k in the subsequent stages of the processing from Section 7.6.2 onwards in the PHT Handbook [2].
For some chopped SS-spectra, including sources with relatively strong emission, there were some pixels which have no flux assigned to them. This occurs because in the original implementation of the DERIVE_SPD software, in staring mode before the implementation of the dynamic flux calibration, it was possible under certain conditions for there to be negative signals leading to negative flux densities. Rather than have negative fluxes in the spectra, the values were set to zero and a flag was set indicating that the fluxes were undefined. For the chopped spectra, where the source spectrum is determined from the difference between on and off target spectra, negative signals are to be expected. It was possible for negative signals to arise in all chopper cycles for a pixel leading to it being flagged as having an undefined flux when the actual flux density is valid. Therefore, the code was modified to allow the full processing of negative signals for chopped mode spectroscopy.
Also in writing the SPD records, a check was made on the source flux densities for negative values, which were instead set to zero. This check has been removed and the actual values are now written to the file.

4 Comparison of Test Cases

5 Consistency Check of Calibration Method with Calibration Standards

Summary

- Chopped mode spectroscopy was successfully revalidated.
- The use of the bi-weight mean algorithm has produced continuum spectra which are smoother and closer to the model spectra than for OLP 10.
- From measurements of standard stars we derive an absolute accuracy of better than $\pm 5\,\%$ for the flux range of $2 - 15\,\mathrm{Jy}$ with the SS-array and $0.4 - 4\,\mathrm{Jy}$ with the SL-array. Some pixels show outliers outside this accuracy range.

5.1 PHT40 Spectroscopy: Consistency Check of Chopped PHT-S Relative Spectral Response Function on Calibration Stars for Different Chopper Modes

5.1.1 Motivation

The measurements of two calibration stars (HR 6817 and HR 6847) were processed and compared. These stars were used to establish the Relative Spectral Response Function (RSRF) for chopped PHT-S measurements and to check whether the input model SED is reproduced. Both calibration stars were measured both in rectangular chopped and triangular chopped mode. This provides an assessment of the consistency between the processing of the two chopper modes.

5.1.2 Method

We compare the results of both OLP 10 and OLP PHTRP001 with the flux models by Hammersley et al. 1998 [3].

5.1.3 Results

Figs. 2 to 5 show individual comparisonsw of both OLP versions with the flux model for each chopped observing mode.
For HR 6817, one can see that the OLP PHTRP001 results show very good agreement between the observations in the two observing modes. Compared to the OLP 10 results, the scatter in the SL-array spectrum is significantly less. However, although there is good agreement with the model to within ∼5-10 %, there is a significant difference in the shape of the SS-array spectrum compared to the model at 3μm, possibly due to absorption by H_2O. There also appears to be a difference ∼5-10 % in the absolute level of the SS-array for the rectangular mode observations compared to the triangular mode, presumably due to a change in resposivity. For the SL-array, the consistency with the model is about 5 % absolute out to about 9μm beyond which the noise makes a significant contribution.
For HR 6847 measured in rectangular chopped mode, one can see that the OLP PHTRP001 spectrum provides a much smoother continuum compared with OLP 10. For the SS-array below 4μm, the consistency with the model is about 5 % absolute and 10-15 % beyond 4μm. For the SL-array, again the consistency with the model is about 5 % absolute, excluding a few outliers out to 9μm, which corresponds to a flux for HR 6487 of $\sim 2 \times 10^{-14}\,\mathrm{W\,m^{-2}}$.
For HR 6847 measured in triangular chopped mode, again the OLP PHTRP001 spectrum is an improvement over the OLP 10 spectrum, since the consistency with the model is better than 5 % absolute and better than ±5 % in relative spectral shape, compared to 10 % for both for OLP 10, excluding some outliers at wavelengths $> 9\mu$m.

5.1.4 Conclusions

- The OLP PHTRP001 gives significantly better results than OLP 10. In each case, the continuum is smoother and closer to the model spectrum.
- There is no significant difference in the results recognizable between rectangular and triangular chopped mode.
- The absolute accuracy was found to be better than 5 % and the relative spectral shape better than ±10 %, although this may, in the case of HR 6817, be due to a spectral feature not taken into account in the model.
- There are fewer outliers compared to OLP 10, although the effects of noise is apparent in the part of the spectrum with low signal to noise, that is $> 9\mu$m.

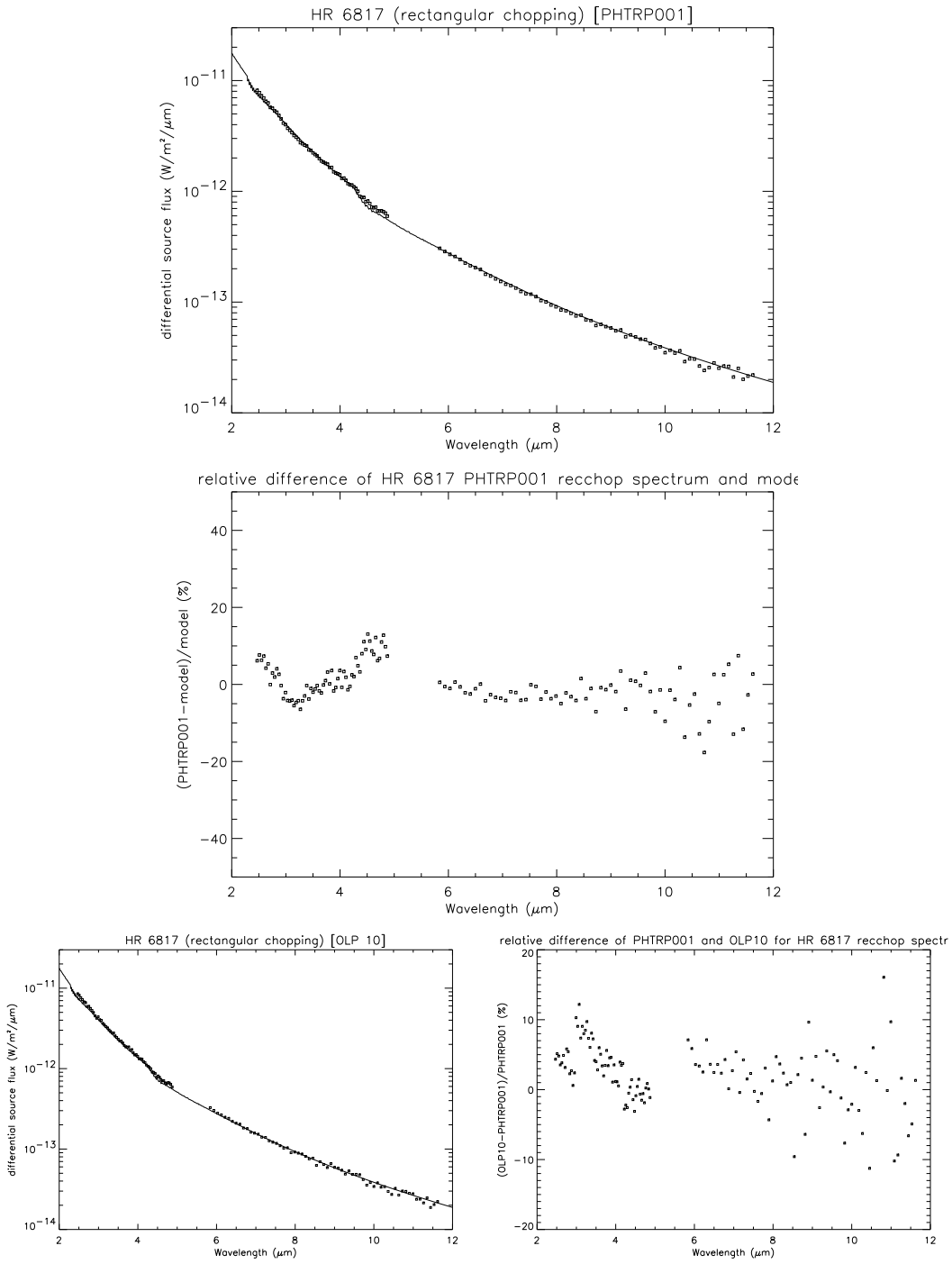

Figure 2: Comparison of the spectrum of HR 6817 obtained in PHT-S rectangular chopped mode with the flux model by Hammersley. OLP PHTRP001 spectrum (upper panel), relative difference to model (middle panel), OLP 10 spectrum (lower left panel) and relative difference between both OLP versions (lower right panel).

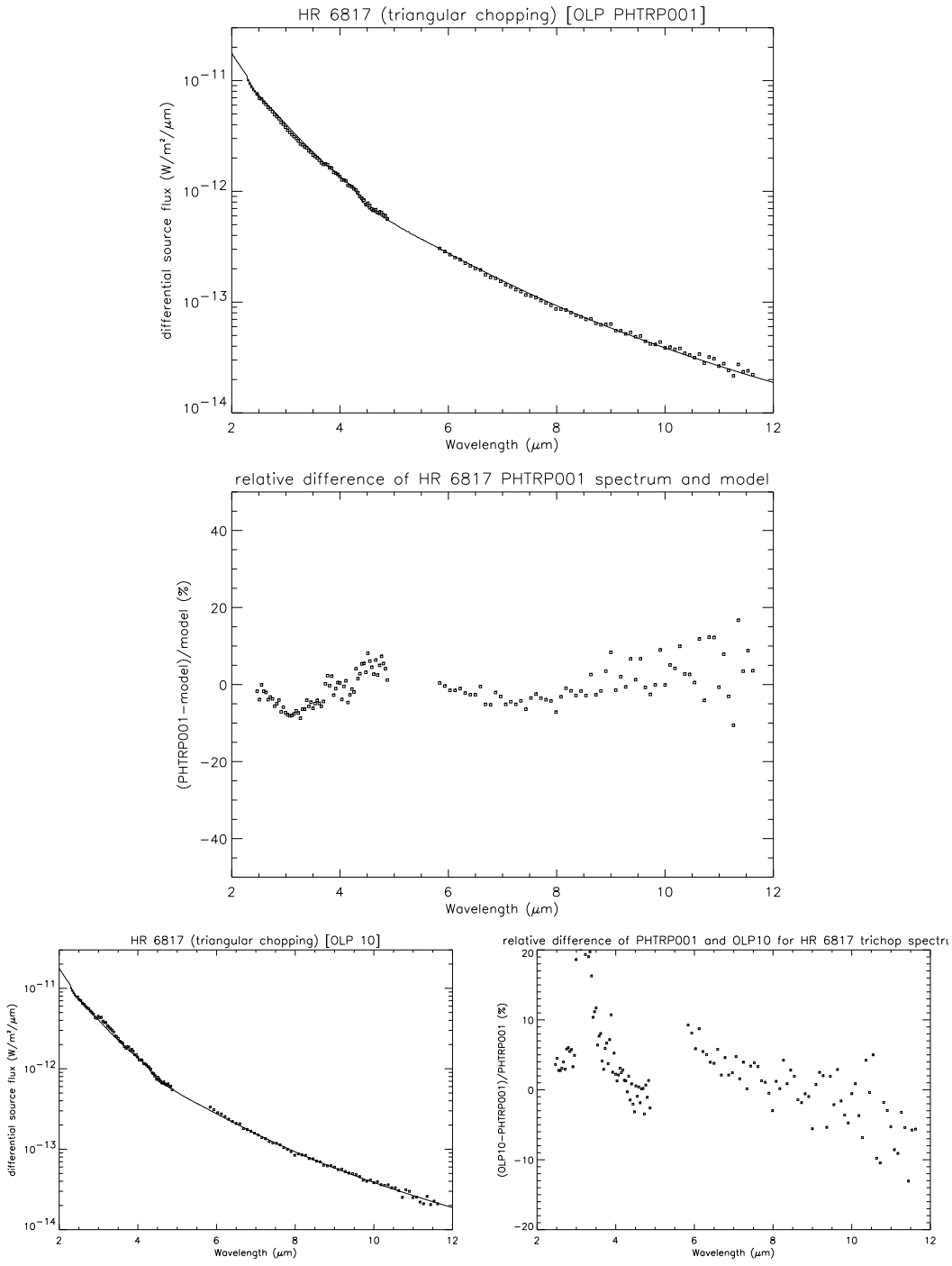

Figure 3: Comparison of the spectrum of HR 6817 obtained in PHT-S triangular chopped mode with the flux model by Hammersley. OLP PHTRP001 spectrum (upper panel), relative difference to model (middle panel), OLP 10 spectrum (lower left panel) and relative difference between both OLP versions (lower right panel).

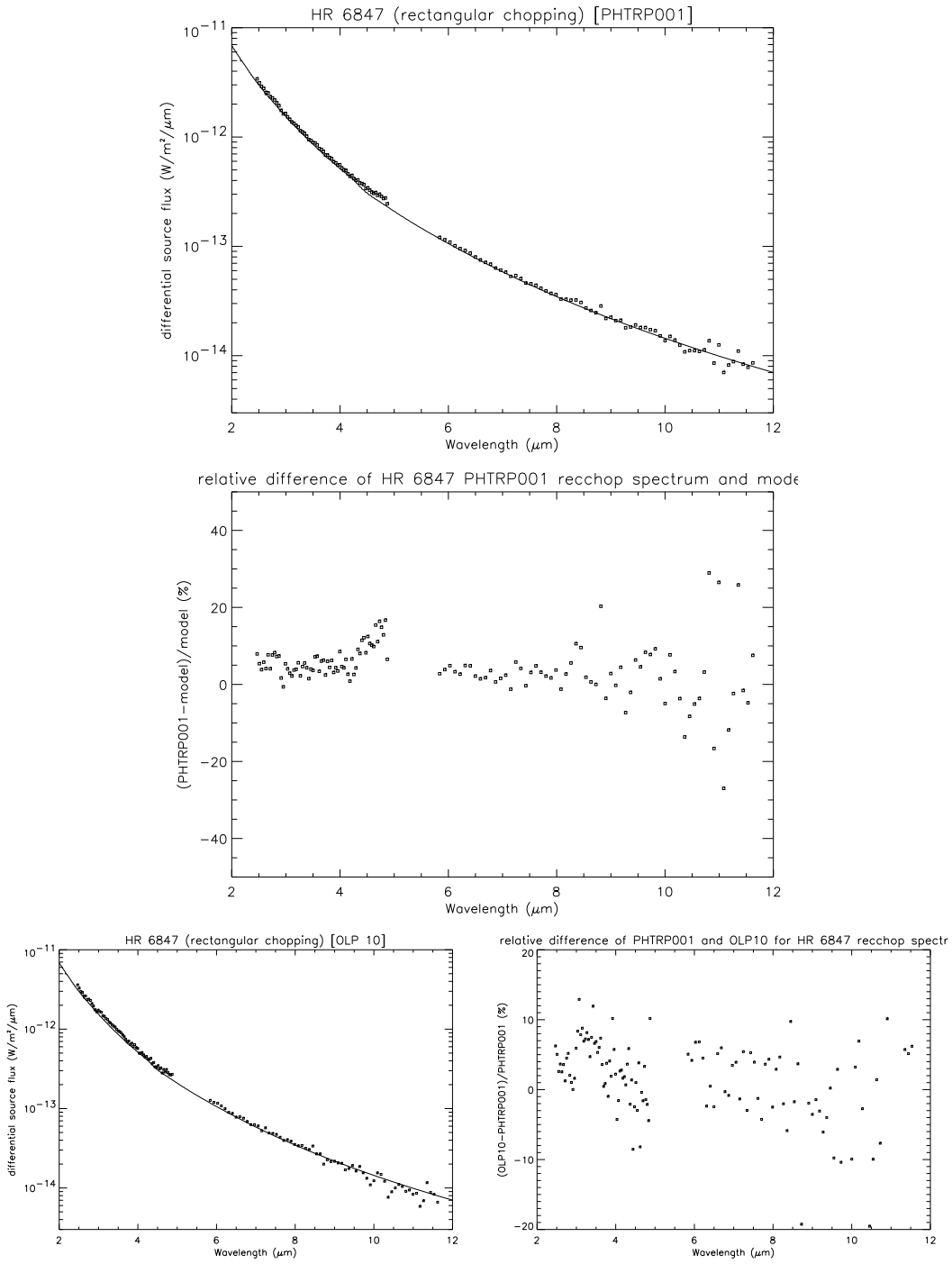

Figure 4: Comparison of the spectrum of HR 6847 obtained in PHT-S rectangular chopped mode with the flux model by Hammersley. OLP PHTRP001 spectrum (upper panel), relative difference to model (middle panel), OLP 10 spectrum (lower left panel) and relative difference between both OLP versions (lower right panel).

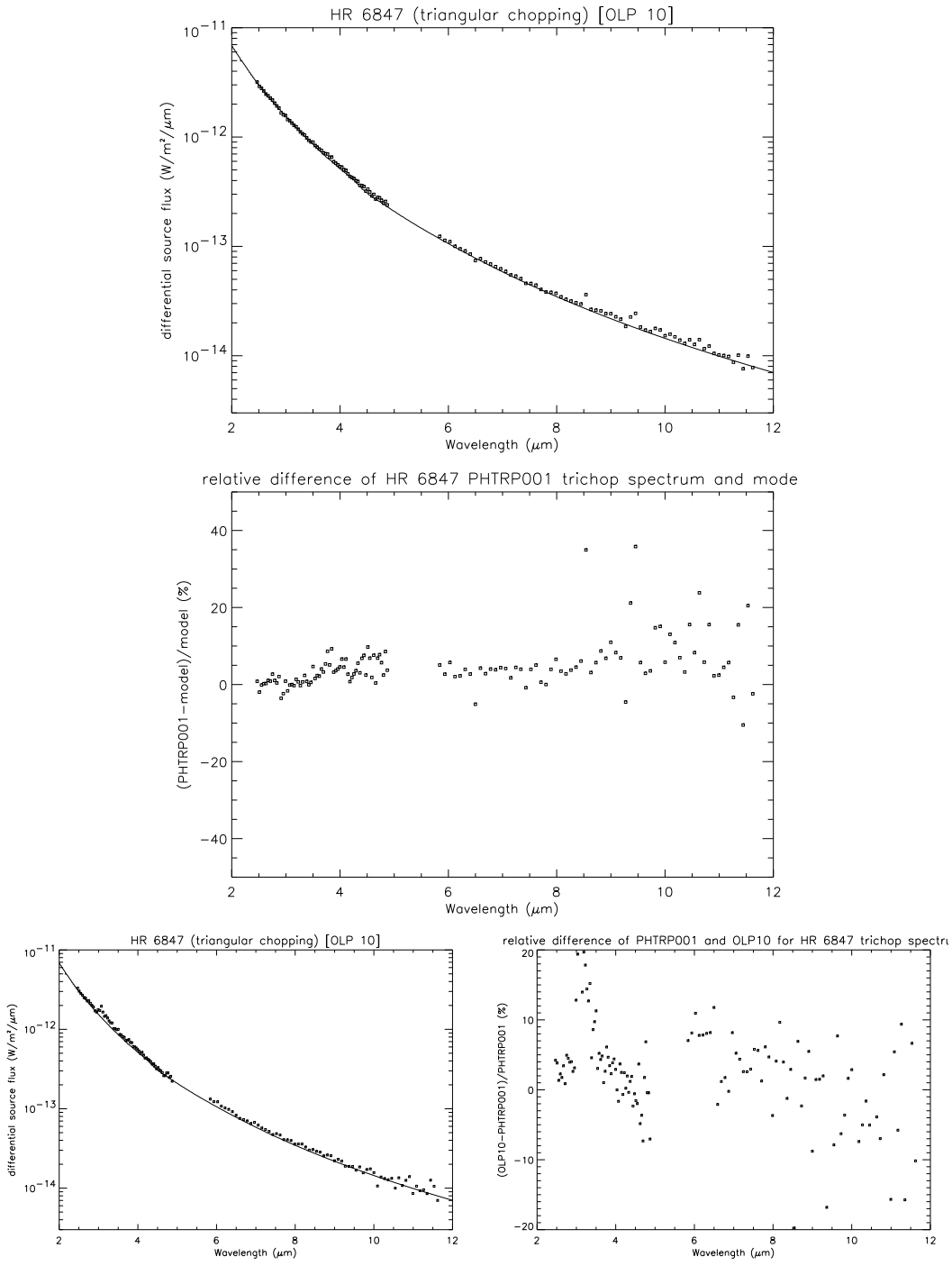

Figure 5: Comparison of the spectrum of HR 6847 obtained in PHT-S triangular chopped mode with the flux model by Hammersley. OLP PHTRP001 spectrum (upper panel), relative difference to model (middle panel), OLP 10 spectrum (lower left panel) and relative difference between both OLP versions (lower right panel).

6 Comparison with Stellar Models for Non-calibration Stars

Summary

- Chopped mode spectroscopy was successfully revalidated.
- For the faint source test cases we find sensitivity limits, when the quality of the calibration accuracy breaks down, of $4 \times 10^{-14}\,\mathrm{W\,m^{-2}\,\mu m^{-1}}$ to $6 \times 10^{-14}\,\mathrm{W\,m^{-2}\,\mu m^{-1}}$ for PHT-SS, corresponding to 300–400 mJy at 4.5 μm, and $6 \times 10^{-15}\,\mathrm{W\,m^{-2}\,\mu m^{-1}}$ to $10^{-14}\,\mathrm{W\,m^{-2}\,\mu m^{-1}}$ for PHT-SL, corresponding to ~150 mJy at 8 μm, for an on-source exposure time of 512 s. These limits should scale approximately with the square root of the on-source exposure time.

6.1 PHT40 Spectroscopy: MIR Spectra of the Stars HD 23763, HR 7428 and HD 23441 from Chopped PHT-S Measurements

6.1.1 Motivation

There are three stars in the data base with similar spectral type as standard stars but different brightness. It is therefore possible to test absolute and relative accuracy of the ISOPHOT-S chopped calibration on different brightness levels than the ones of standard stars used to establish the calibration. The properties of the three stars are compiled in Table 1:

Table 1: Properties of stars used for verification of chopped ISOPHOT-S spectra

Name	Spectral Type	Apparent Brightness (mag)	Comment	Reference Star	Spectral Type	Apparent Brightness (mag)
HD 23763	A1V	m_k = 6.567		Sirius (HR 2491)	A1V	m_k = -1.39
HR 7428 (HD 184398)	K2II-III+A0V Sp(IR) K2II-III Ca-	m_v = 6.37	RS CVn binary	HR 6688	K2III	m_v = 3.747
HD 23441	A0Vn	m_v = 6.43	Pleiades859	Vega (HR 7001)	A0V	m_v = 0.033

For a reference of the spectral types of HR 7428, cf. [8], and of HD 23441, cf. [10]. HR 7428 has an IRAS 12 μm flux of 1.82 Jy, cf. [9] (=1.26 Jy for T=4000 K BB).

6.1.2 Method

The model spectra of Sirius, HR 6688 and Vega are scaled according to the apparent brightness ratio in the K or V band. The absolute fluxes and relative shapes of the ISOPHOT-S spectra of both OLP 10 and OLP PHTRP001 are compared with the scaled model spectra.

6.1.3 Results

In Figs. 6 to 8 we perform an individual comparison of both OLP versions with the flux model. One can see that the results are practically identical.
For HD 23763 the PHT-SS fluxes out to 4 μm fulfill the criterium with absolute accuracy ~5-10 % and relative accuracy <10 %. Below a flux level of 4.2×10^{-14} W m^{-2} μm^{-1}, corresponding to TBD mJy at 4.5 μm, a larger scatter with higher uncertainties occurs. For PHT-SL there is good performance up to 8 μm. Below a flux level of 6×10^{-14} W m^{-2} μm^{-1}, corresponding to TBD mJy at 8 μm there is again a larger scatter with higher uncertainties. These appear to be sensitivity limits. The on-source exposure time was 512 s.
HR 7428 is a factor of 10 brighter than HD 23763. There is a systematic constant offset between the measurement and the scaled model, so that it remains open whether this is totally due to calibration or also due to some uncertainty in the brightness ratio. For OLP PHTRP001, the relative spectral shape is better than ±5 %, compared to ±10 % for OLP 10.
HD 23441 is a similar case as HD 23763. For the SS-array there is good agreement with the model except for a few pixels at the long wavelength end. This is in contrast with the OLP 10 spectrum where the good calibration accuracy is lost at 4 μm and beyond. For the SL-array, the PHTRP001 spectrum is smoother to 7 μm and there appears to be emission features, possibly from the 7.7 μm and 8.6 μm PAH features, although at 9 μm (corresponding to a flux level of $\sim 4^{-14}$ W m^{-2} μm^{-1}) and beyond the spectrum is affected by noise. Again the on-source exposure time was 512 s. .

6.1.4 Conclusions

- The OLP PHTRP001 version again gives better results. The continuum is smoother and the absolute accuracy is better than the 10 % accuracy for OLP 10.
- These faint source test cases probe sensitivity limits for this measurement mode which are 4×10^{-14} W m^{-2} μm^{-1} to 6×10^{-14} W m^{-2} μm^{-1}, corresponding to 300-

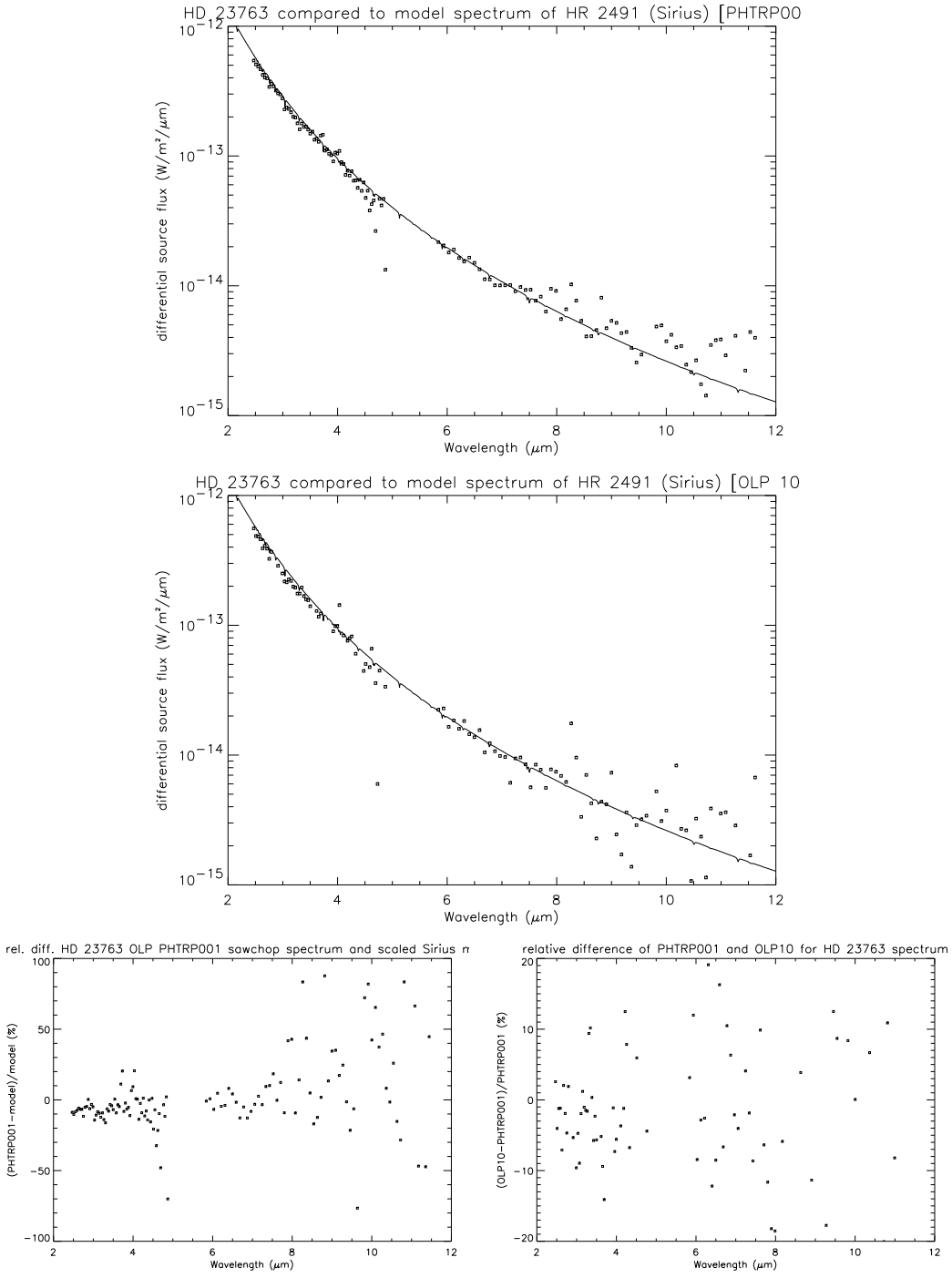

Figure 6: Comparison of the spectrum of the A1V star HD 23763 obtained in PHT-S sawtooth chopped mode with the model of Sirius scaled with the K-magnitude ratio of (6.567 mag / -1.39 mag) for both OLP PHTRP001 (upper panel) and OLP 10 (middle panel) and the relative difference to the model and both versions (lower panel).

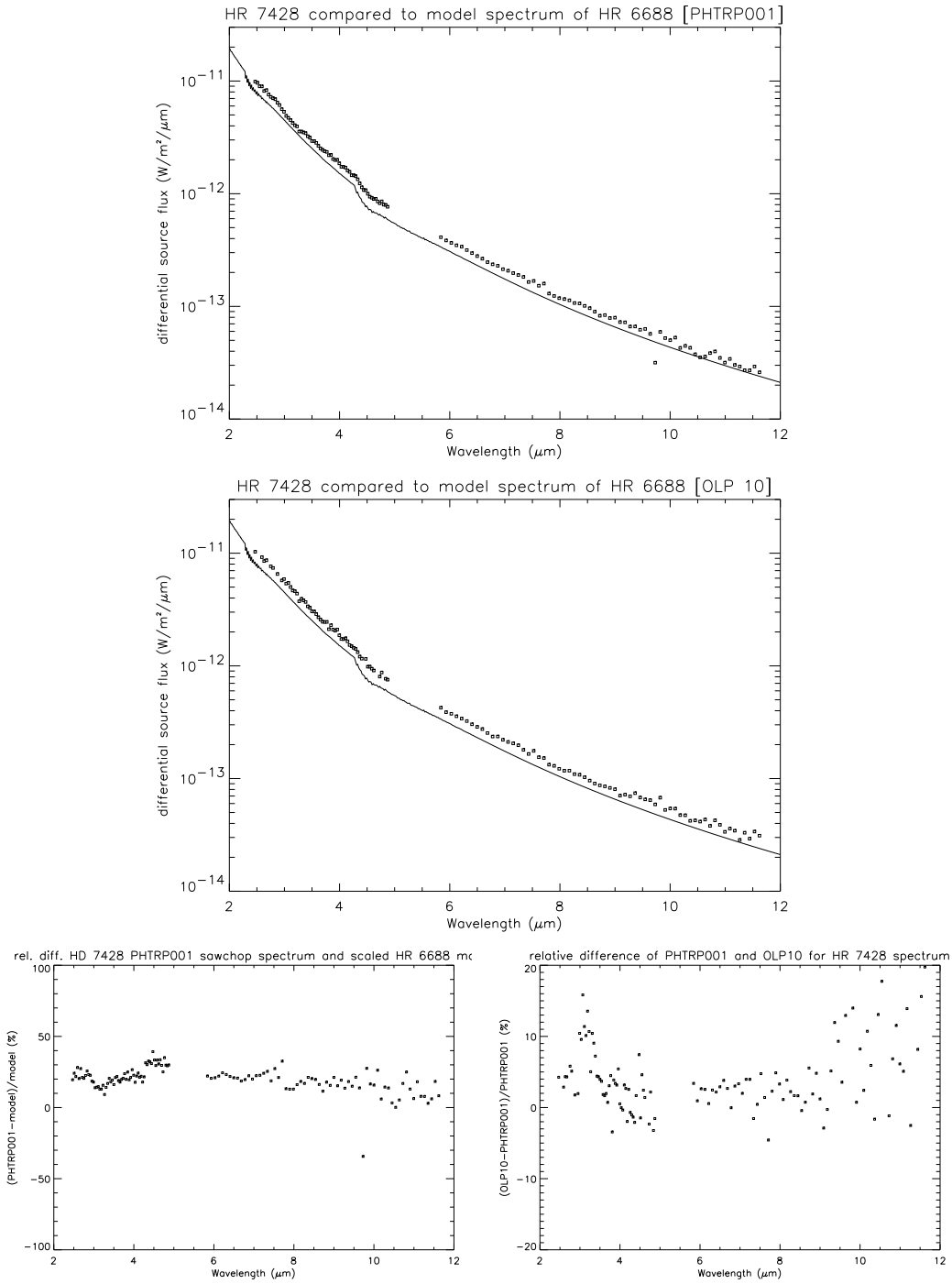

Figure 7: Comparison of the spectrum of the RS CVn binary HR 7428 (spectral type: K2II-III+A0V) obtained in PHT-S rectangular chopped mode with the model of HR 6688 (spectral type: K2III) scaled with the V-magnitude ratio of (6.37 mag / 3.747 mag) for both OLP PHTRP001 (upper panel) and OLP 10 (middle panel) and the relative difference to the model and both versions (lower panel).

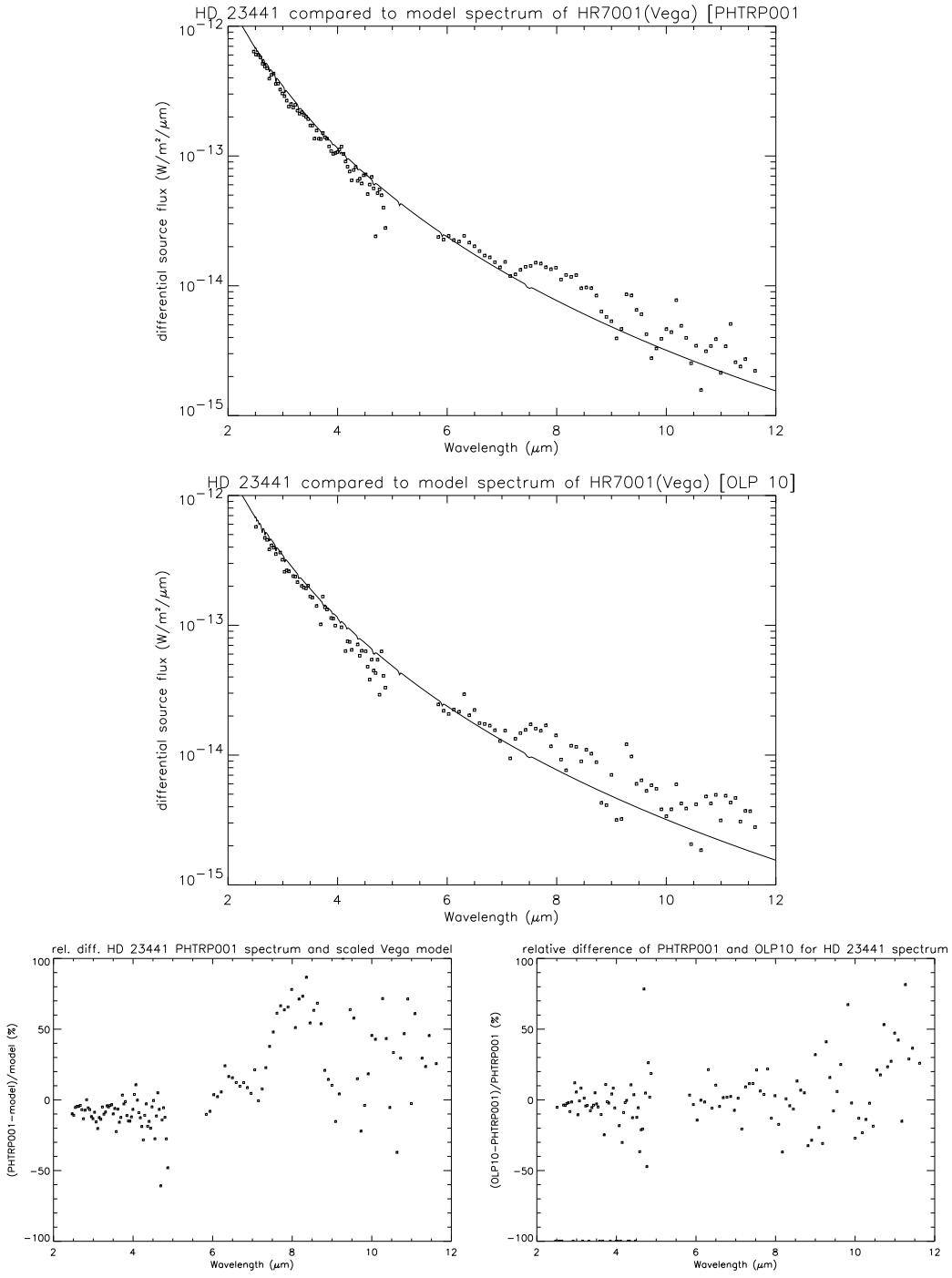

Figure 8: Comparison of the spectrum of the A0Vn star HD 23441 obtained in PHT-S saw-tooth chopped mode with the model of Vega scaled with the V-magnitude ratio of (6.43 mag / 0.033 mag) for both OLP PHTRP001 (upper panel) and OLP 10 (middle panel) and the relative difference to the model and both versions (lower panel).

400 mJy at 4.5 μm, and 6×10^{-15} W m^{-2} μm^{-1} to 10^{-14} W m^{-2} μm^{-1}, corresponding to $\sim$150 mJy at 8 μm, for an on-source exposure time of 512 s.

7 Comparison with Ground-based Spectroscopy

Summary

- Chopped mode spectroscopy was successfully revalidated.
- The use of the bi-weight mean algorithm produces continuum spectra which are smoother allowing clear identification of PAH features and atomic lines in the galaxy spectra.
- There is a quite good consistency with ground-based spectroscopy, in particular w.r.t. spectral features. A 1-to-1 correspondence, in particular in absolute level, does not have to be expected due to the quite different beam sizes and the extension of several targets.
- The galaxy spectra confirm the findings for stellar spectra that sensitivity limits of accurate spectrophotometry for typically 512 s on-source exposure time are around $7 \times 10^{-14}\,\mathrm{W\,m^{-2}\,\mu m^{-1}}$ for PHT-SS, corresponding to around 400 mJy at $4\,\mu$m and $5 \times 10^{-15}\,\mathrm{W\,m^{-2}\,\mu m^{-1}}$ for PHT-SL, corresponding to $\sim$110 mJy at $8\,\mu$m.
- On rare occasions, a pixel is affected by a very high energy particle and consequently the flux is significantly above (e.g.Mrk 463) or below the continuum (e.g Mrk231), which could be mistaken for narrow emission or absorption features.

7.1 PHT40 Spectroscopy: MIR Spectra of a Symbiotic Star from Chopped PHT-S Measurements

7.1.1 Motivation

In order to to increase the variety of object types for which PHT-S spectra are checked we included the spectrum of a symbiotic star, AG Peg in our test case list. Groundbased 8 - 13 micron spectroscopy is available (cf. Refs. [6]).

7.1.2 Method

We compare the absolute fluxes and relative shapes of the ISOPHOT-S spectra of both OLP PHTRP001 and OLP 10 with the groundbased spectroscopy. Note that we compare an aperture size of 24x24 arcsec^2 for ISOPHOT-S with 5 arcsec aperture size of the groundbased measurements.

7.1.3 Results

In Fig. 9 we perform an individual comparison of both OLP versions with the flux model. Both OLP versions show practically identical results and there is a good agreement with the ground-based spectroscopy.

7.1.4 Conclusions

- The two OLP versions give very similar results.
- For the symbiotic star AG Peg we find a good consistency with ground-based $8 - 13\,\mu$m spectroscopy.

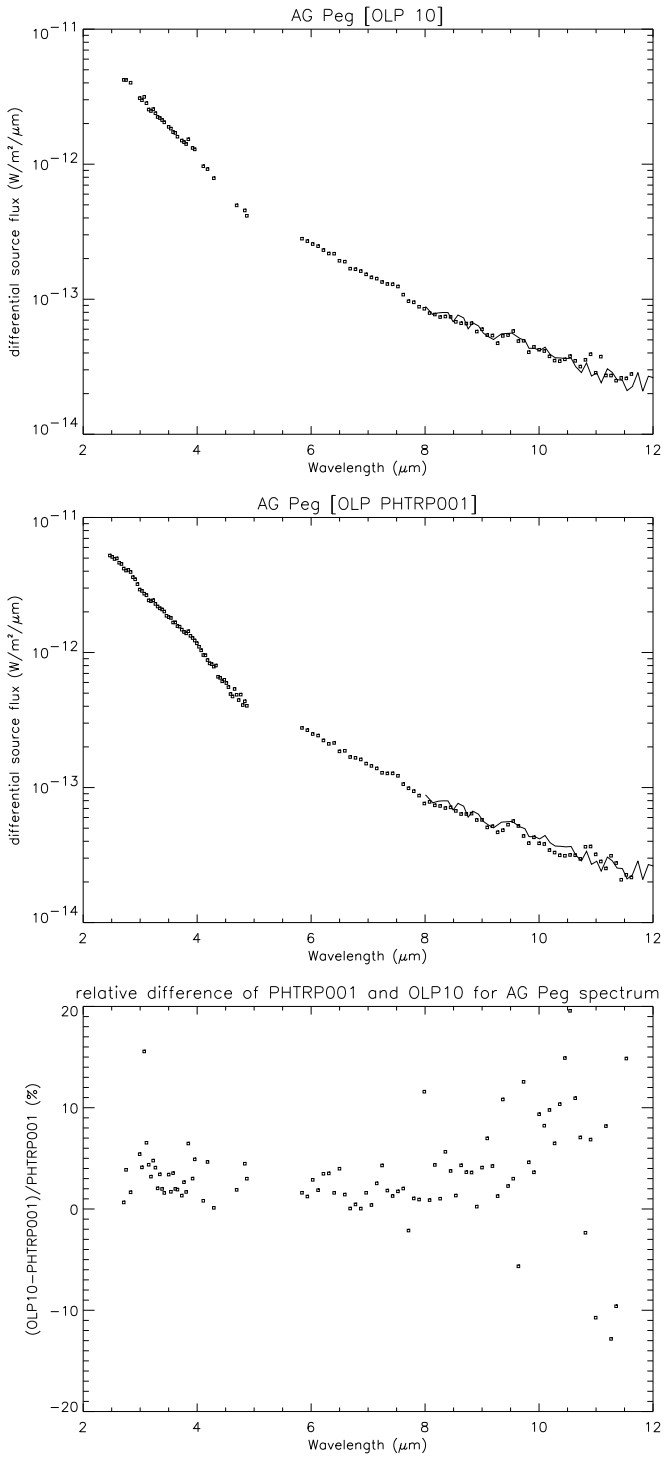

Figure 9: Comparison of the spectrum of the symbiotic star AG Peg obtained in PHT-S triangular chopped mode with the groundbased 8 – 13 micron spectroscopy by Roche et al. 1983 for both OLP 10 (upper panel) and OLP PHTRP001 (middle panel) and the relative difference of both versions (lower panel).

7.2 PHT40 Spectroscopy: MIR Spectra of Galaxies from Chopped PHT-S Measurements

7.2.1 Motivation

There is a set of chopped PHT-S measurements of galaxies with fluxes in the range 10^{-14} to $10^{-12}\,\mathrm{W/m^2/\mu m}$. These galaxies have different SED shapes than the standard stars from which the chopped PHT-S spectral response function was derived. There is groundbased 8 – 13 micron spectroscopy available (cf. Ref. [5]). We selected a range of galaxies from featureless continuum to spectra with PAH features and strong 10 μm silicon absorption.

7.2.2 Method

We compare the absolute fluxes and relative shapes of the ISOPHOT-S spectra of both OLP 10 and OLP PHTRP001 with the groundbased spectroscopy. Note that we compare an aperture size of 24x24 arcsec^2 for ISOPHOT-S with 5 arcsec aperture size of the groundbased measurements. Note, that in previous reports there appeared to be an inconsistency for NGC 5253 with the groundbased spectrum showing a higher flux than the ISOPHOT-S spectrum. This could be traced back to a wrong flux level scaling (a factor 10 too high) in Roche et al. (1991) by looking up the spectrum of the source in Aitken et al. (1982, MNRAS 199, 31P).

7.2.3 Results

In Figs. 10 to 26 we perform an individual comparison of both OLP versions with the ground-based spectroscopy. The spectra are ordered with increasing PAH and silicate absorption feature strength.
NGC 1068 is by far the brightest object of the sample considered here. NGC 1068, NGC 4151, NGC 5506, Mrk 231 and 3C 273 are the only galaxies with 2.5 – 4 μm fluxes being above $7 \times 10^{-14}\,\mathrm{W\,m^{-2}\,\mu m^{-1}}$ and hence above the sensitivity limit for PHT-SS. For all the other galaxies the PHT-SS channel displays only noise. The PHT-SL spectra show a very good agreement in the relative spectral shape with the ground-based spectroscopy. In some cases the PHT-SL spectrum shows a significantly higher flux indicating the extension of the source (3C 273 is a variable source).
There follows a description of the individual sources illustrating some of the spectral features:
NGC 1068 The PHTRP001 spectrum is smoother over the whole wavelength range. There are weak 7.7 and 8.6μm PAH features, with the possibility that the faint peak at 11.3μm could also be due to PAHs. There is also evidence for the [SIV] line at 10.5μm.
NGC 4151 The smoother PHTRP001 spectrum appears to be somewhat featureless as is the groundbased 8-13μm spectrum.
NGC 5506 The PHTRP001 spectrum shows strong silicate absorption which is also apparent in the OLP 10 spectrum. However, the smoother spectrum again shows weak PAH features at 6.2, 7.7 and 11.3μm. There is also evidence of very faint PAH emission at 8.6μm which is obscured by the slope of the silicate feature. The [SIV] line at 10.6μm is prominent as in the groundbased 8-13μm spectrum and there is evidence of the redshifted [ArII] and [ArIII] lines around 7 and 9μm respectively.
Mrk 463 The smoother PHTRP001 SL spectrum shows evidence of several emission line features. The line at 9.5μm corresponds to the (redshifted) [ArIII] line. However, the feature at 11.1-11.2μm does not quite fit the central wavelength of the redshifted [SIV] line, which should be present if the [ArIII] line is excited. In addition, the bright feature at 8.8μm does not correspond to any known emission line feature. The continuum for this source is very faint and the features are $\sim 3\sigma$. A detailed examination of the raw data associated with the pixels showed that for the 8.8μm pixel and the pixel corresponding to the [ArIII] line, the on-source pointing in the last chopper cycle was affected by high energy particles. This significantly increased the responsivity for the whole of this part of the cycle, making the average value over all cycles significantly higher than for adjacent pixels.
NGC 1275 The PHTRP001 SL spectrum is much smoother than OLP 10 and there are weak 6.2, 7.7 and 8.6μm PAH features. It is possible that the weak feature at 7.1μm is the [ArII] line. The peak in the groundbased 8-13μm spectrum at 8.2μm is not reproduced in the SL spectrum.

3C 273 The spectrum is featureless and somewhat smoother in the SS part. The higher groundbased 8-13μm spectrum can be attributed to the variability of this source.
NGC 3783 Although the PHTRP001 SL spectrum is much smoother than OLP 10, the continuum is not smooth enough to identify any narrow band features.
I Zw 1 Again, although the PHTRP001 SL spectrum is smoother, it is not possible to make a clear indentification of narrow band features.
NGC 4051 The spurious outliers in the OLP 10 spectra do not appear in the PHTRP001 product. The PHTRP001 SL spectrum shows faint PAH features at 6.2, 7.7, 8.6 and 11.3μm. There are also a strong emission line feature at 10.6μm ([SIV]), but the feature at 9.2μm is too far from the expected redshifted wavelength of 9μm for [ArIII].
NGC 5253 The smoother PHTRP001 SL spectrum shows strong PAH emission features at 6.2, 7.7 and 8.6μm and silicate absorption at 9μm and beyond which there is a weak PAH feature at 11.3μm. There are also strong emission lines from [SIV] at 10.5μm, which is also seen in the groundbased 8-13μm spectrum, and [ArIII] at 9μm.
NGC 4388 The PHTRP001 spectrum shows strong PAH emission features at 6.2 and 7.7μm and strong silicate absorption in which the continuum is too noisy to distinguish the longer wavelength PAH features and atomic lines.
Mrk 231 The PHTRP001 SL spectrum is smoother showing (redshifted) 6.2, 7.7 and 8.6μm PAH features and silicate absorption. Note that there is a spectral point at 10.5μm which is significantly below the continuum. This was caused by a very high energy particle which resulted in a change in responsivity for most of the off-source part of a cycle. As there are only two on-off source cycles for this observation, this reduced the on-off source signal difference compared to the values for adjacent pixels.
NGC 4102 The PAH features at 6.2, 7.7, 8.6 and 11.3μm are relatively strong for this source, which also has a stong silicate absorption feature.
Mrk 331 (1) & (2) There are two spectra for this source which are consistent and shw prominent 6.2, 7.7, 8.6 and 11.3μm PAH features and silicate absorption. There is also evidence of emission from the [ArII] line at 7μm in both spectra. The spectrum is noisy in the silicate absorption region making the identification of the [ArIII] and [SIV] lines difficult.
NGC 4418 There is a strong silicate absorption feature in the spectrum which is in very good agreement with the groundbased 8-13μm spectrum. The PHTRP001 spectrum is very similar to that of OLP 10 and shows no obvious PAH emission features.
Arp 220 There is a strong silicate absorption feature in agreement with the groundbased 8-13μm spectrum. Also the 6.2 and 7.7μm PAH features are prominent, but the presence of the longer wavelength PAH features is not so clear.

7.2.4 Conclusions

- The OLP PHTRP001 version gives better results than OLP 10 for all the galaxy spectra examined. The continuum spectra are consistently smoother, which provides clear identification of PAH features and atomic lines.
- The galaxy spectra confirm the findings for stellar spectra that sensitivity limits of accurate spectrophotometry for typically 512 s on-source exposure time are around $7 \times 10^{-14}\,\mathrm{W\,m^{-2}\,\mu m^{-1}}$ for PHT-SS, corresponding to around 400 mJy at 4 μm and $5 \times 10^{-15}\,\mathrm{W\,m^{-2}}\,\mu$m for PHT-SL, corresponding to $\sim$110 mJy at 8 μm.
- On rare occasions, a pixel is affected by a very high energy particle and consequently the flux is significantly above (e.g.Mrk 463) or below the continuum (e.g Mrk231), which could be mistaken for narrow emission or absorption features.

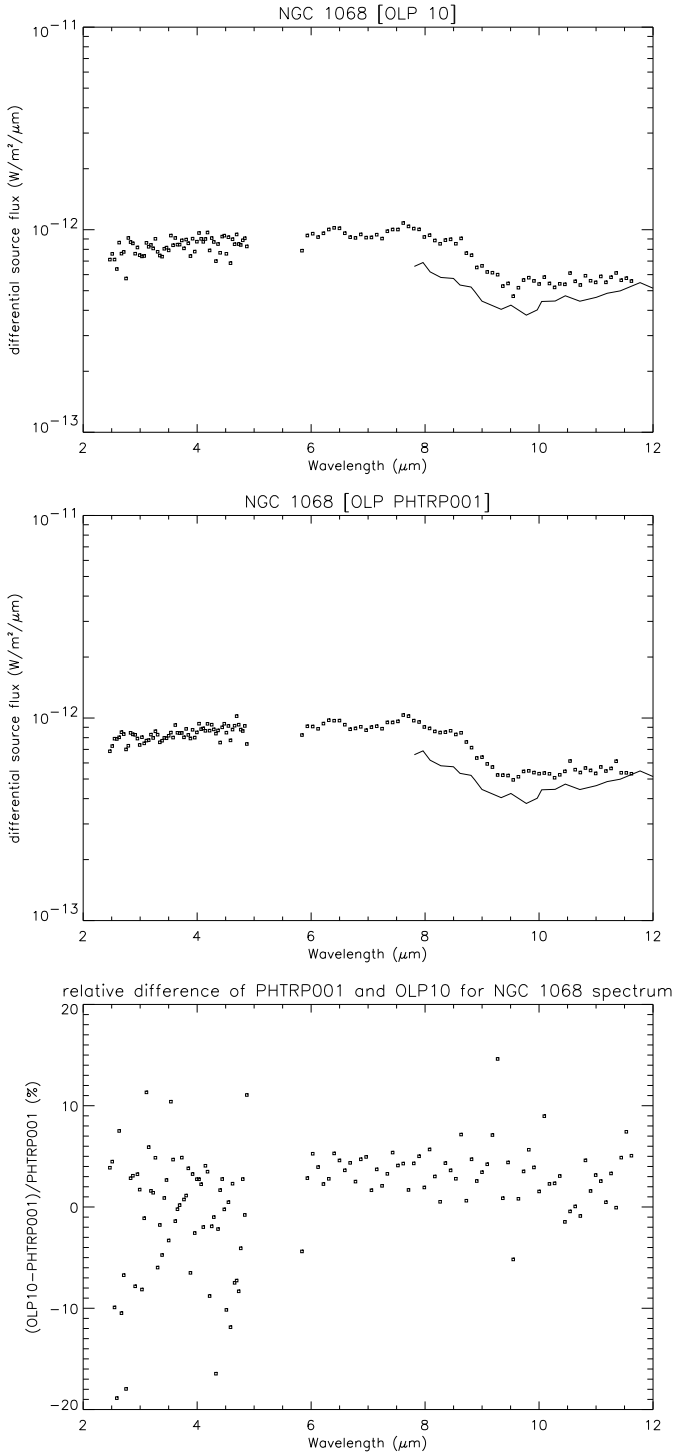

Figure 10: Comparison of the spectrum of NGC 1068 obtained in rectangular chopped mode (dots) with groundbased 8 – 13 micron spectroscopy (solid line) by Roche et al. 1991 for both OLP 10 (upper panel) and OLP PHTRP001 (middle panel) and the relative difference of both versions (lower panel).

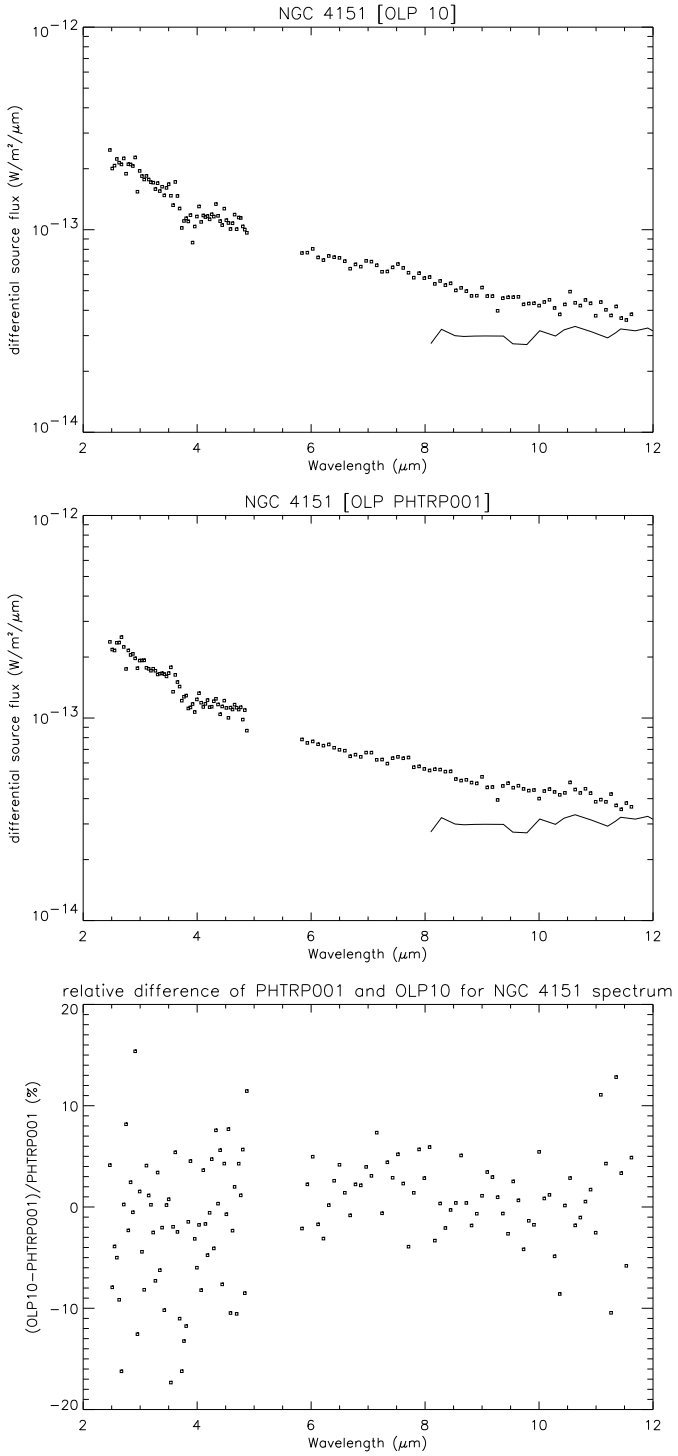

Figure 11: Comparison of the spectrum of NGC 4151 obtained in rectangular chopped mode (dots) with groundbased 8 – 13 micron spectroscopy (solid line) by Roche et al. 1991 for both OLP 10 (upper panel) and OLP PHTRP001 (middle panel) and the relative difference of both versions (lower panel).

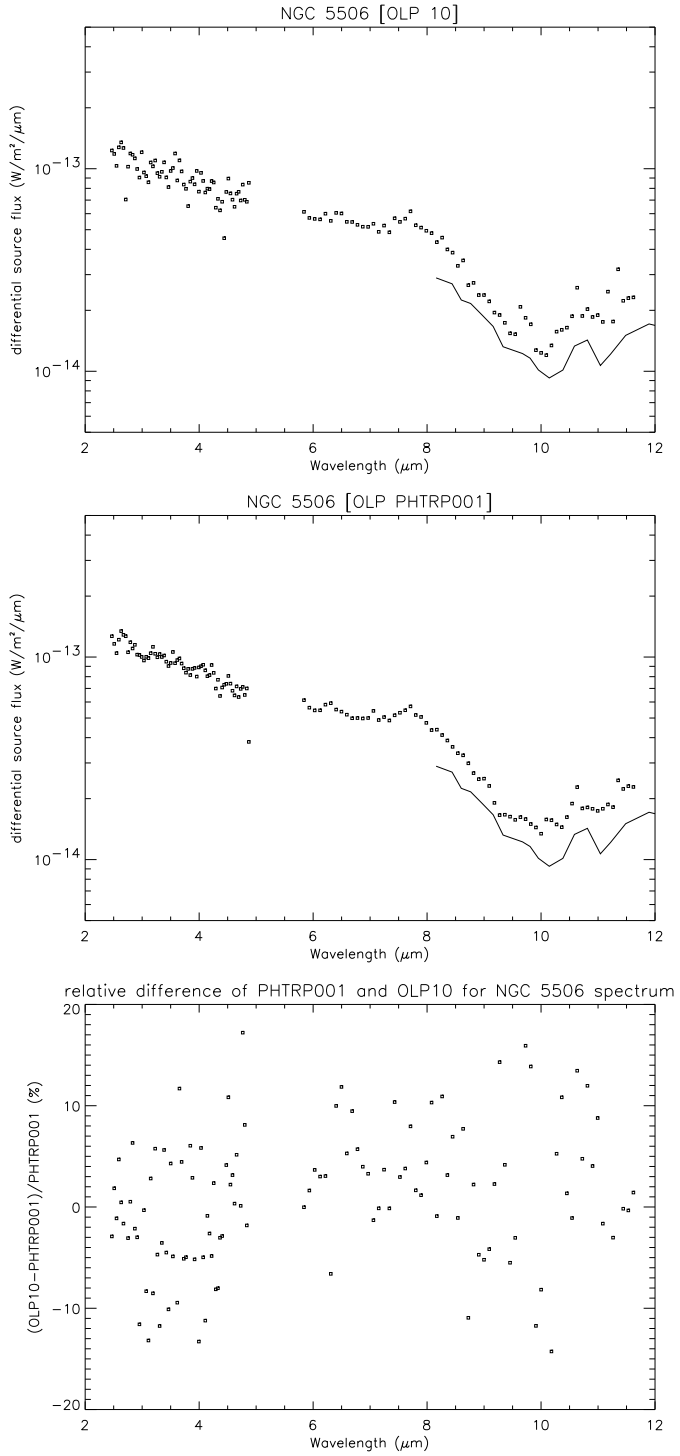

Figure 12: Comparison of the spectrum of NGC 5506 obtained in rectangular chopped mode (dots) with groundbased 8 – 13 micron spectroscopy (solid line) by Roche et al. 1991 for both OLP 10 (upper panel) and OLP PHTRP001 (middle panel) and the relative difference of both versions (lower panel).

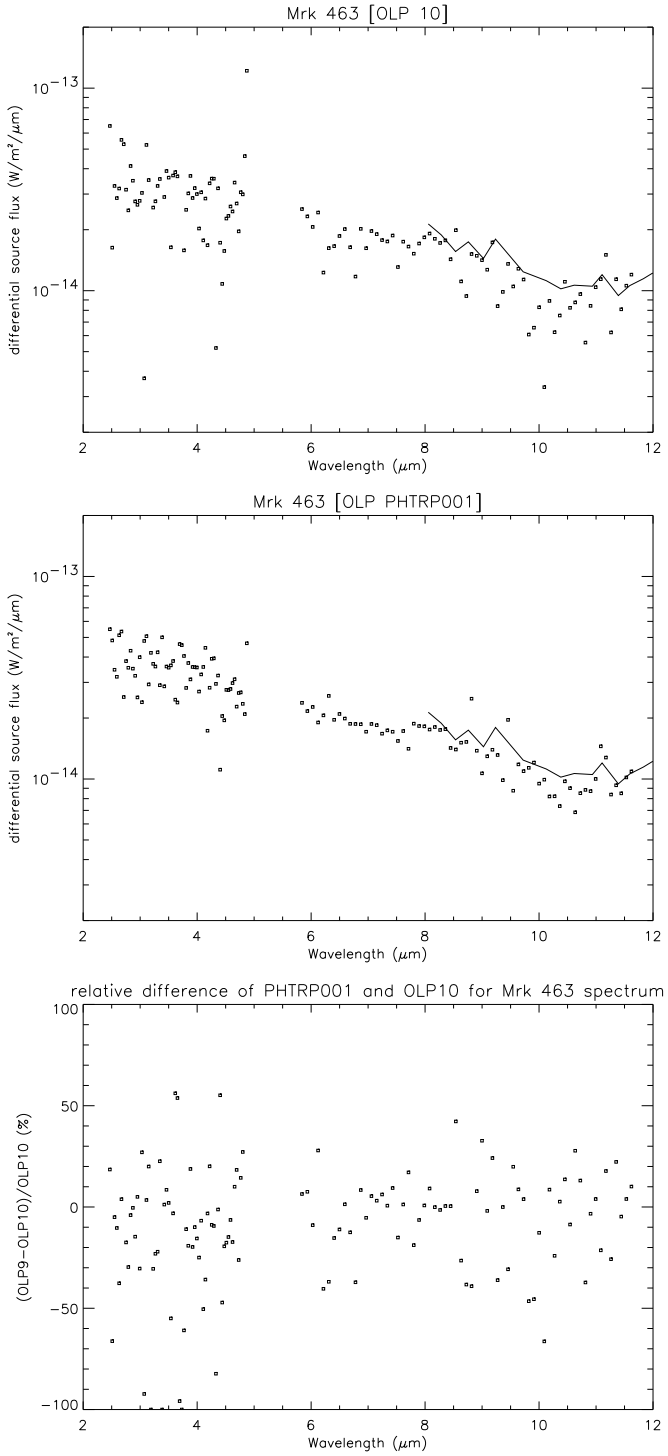

Figure 13: Comparison of the spectrum of Mrk 463 obtained in rectangular chopped mode (dots) with groundbased 8 – 13 micron spectroscopy (solid line) by Roche et al. 1991 for both OLP 10 (upper panel) and OLP PHTRP001 (middle panel) and the relative difference of both versions (lower panel).

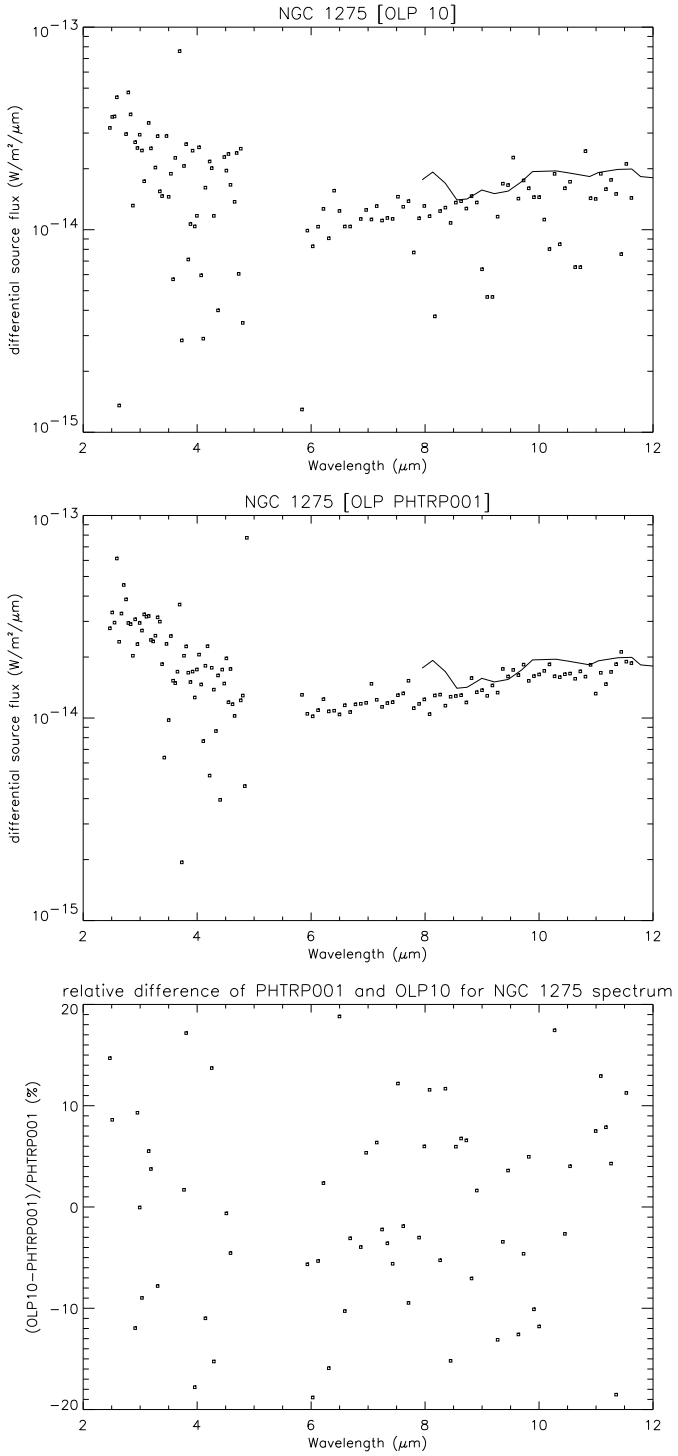

Figure 14: Comparison of the spectrum of NGC 1275 obtained in rectangular chopped mode (dots) with groundbased 8 – 13 micron spectroscopy (solid line) by Roche et al. 1991 for both OLP 10 (upper panel) and OLP PHTRP001 (middle panel) and the relative difference of both versions (lower panel).

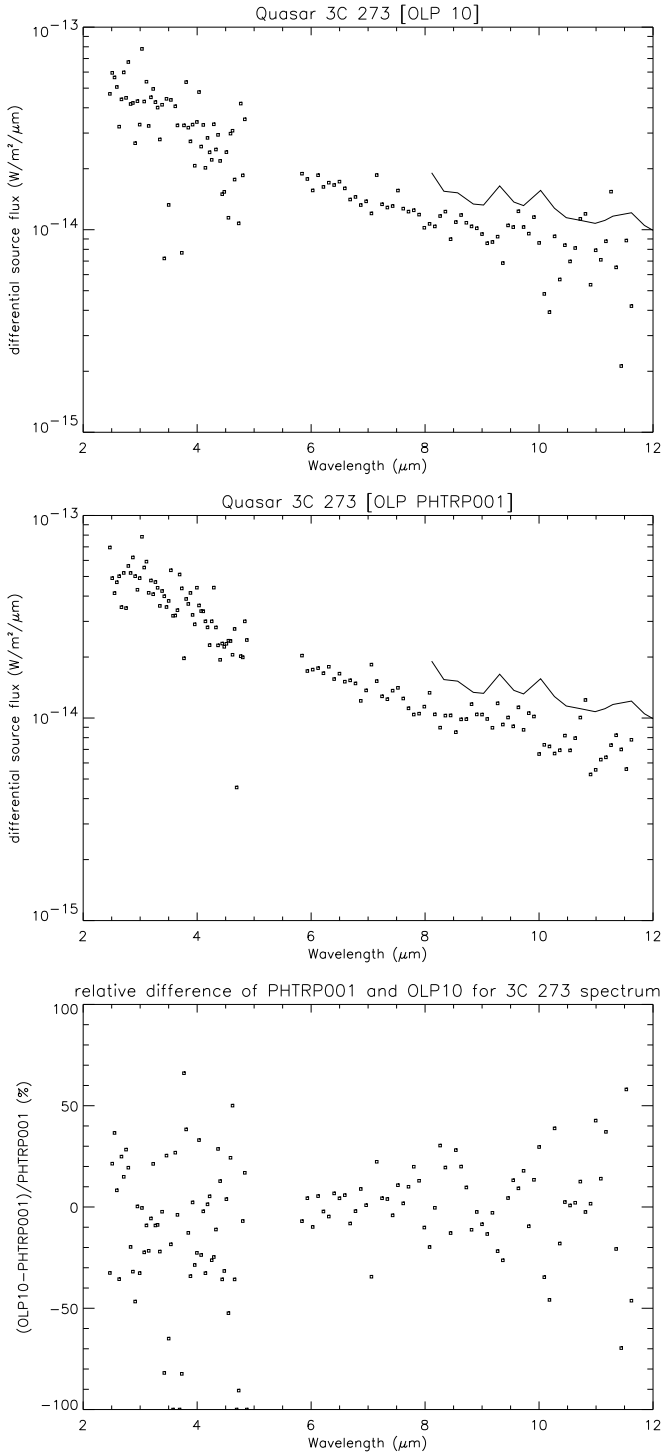

Figure 15: Comparison of the spectrum of 3C 273 obtained in rectangular chopped mode (dots) with groundbased 8 – 13 micron spectroscopy (solid line) by Roche et al. 1991 for both OLP 10 (upper panel) and OLP PHTRP001 (middle panel) and the relative difference of both versions (lower panel).

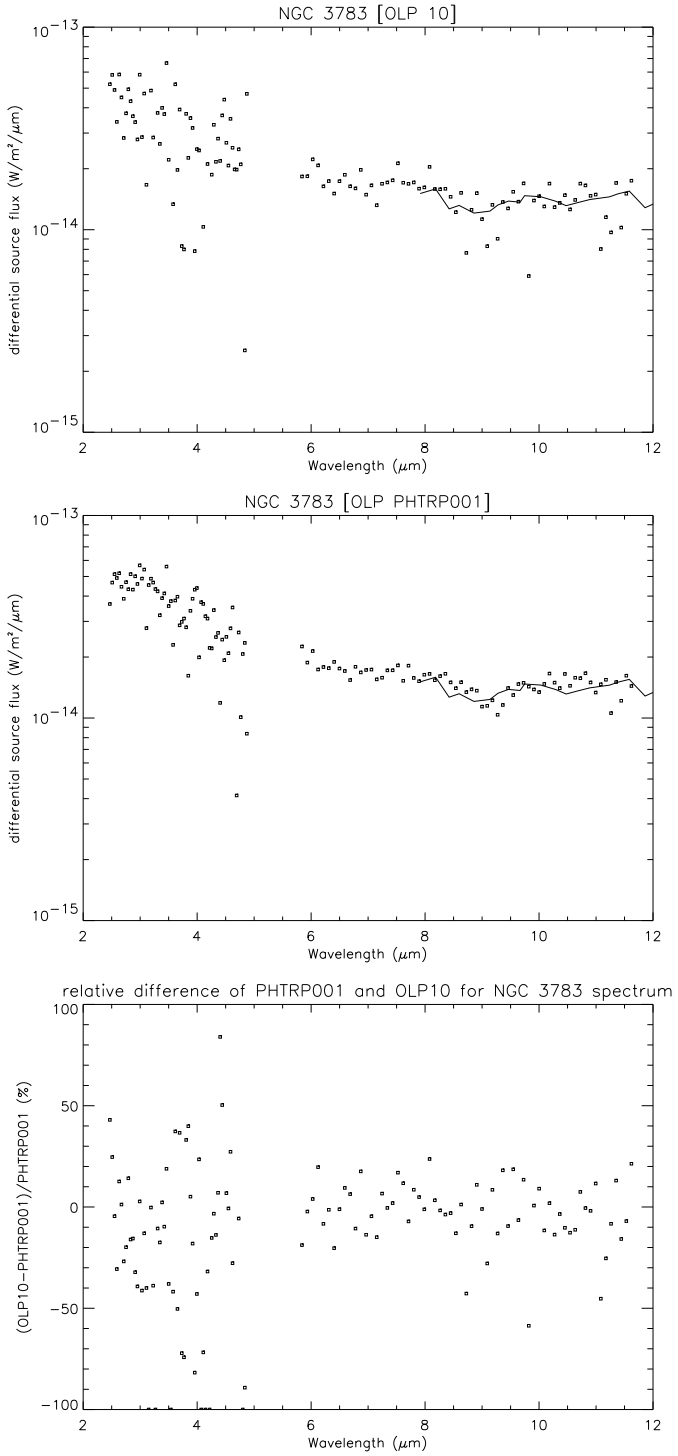

Figure 16: Comparison of the spectrum of NGC 3783 obtained in rectangular chopped mode (dots) with groundbased 8 – 13 micron spectroscopy (solid line) by Roche et al. 1991 for both OLP 10 (upper panel) and OLP PHTRP001 (middle panel) and the relative difference of both versions (lower panel).

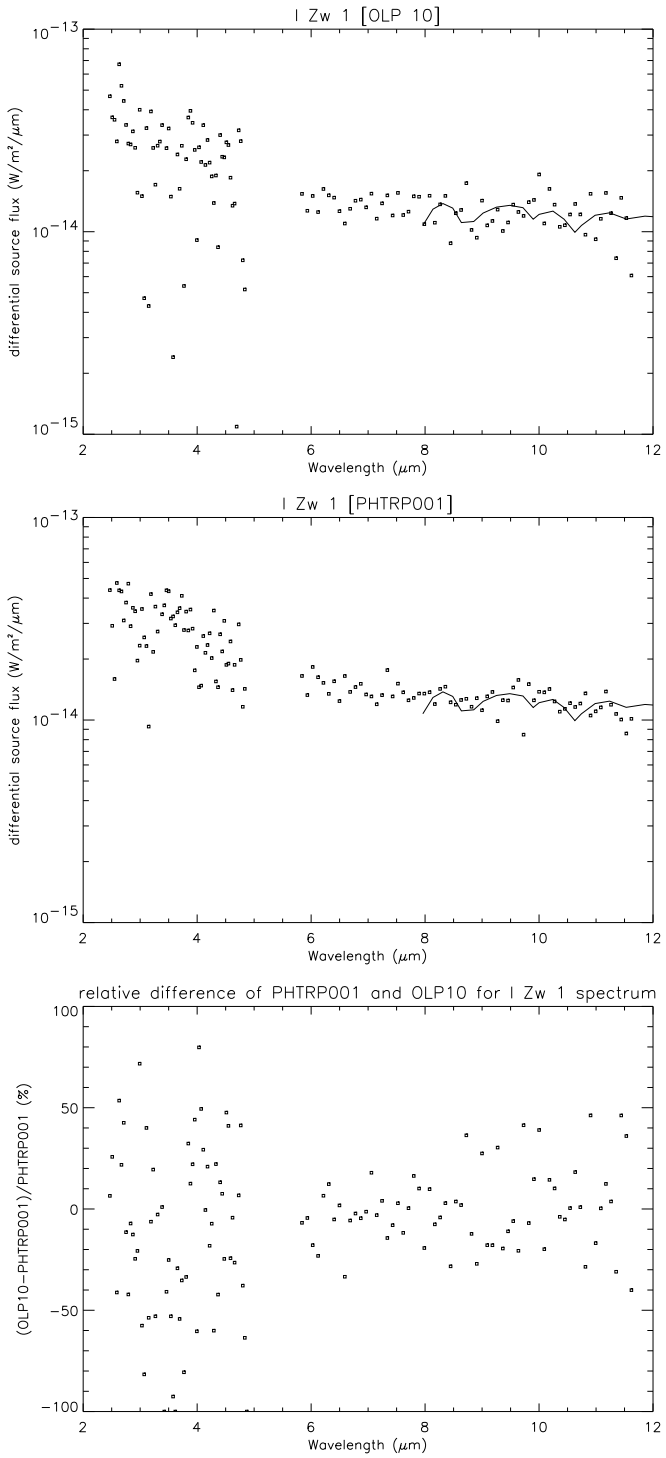

Figure 17: Comparison of the spectrum of I Zw 1 obtained in rectangular chopped mode (dots) with groundbased 8 – 13 micron spectroscopy (solid line) by Roche et al. 1991 for both OLP 10 (upper panel) and OLP PHTRP001 (middle panel) and the relative difference of both versions (lower panel).

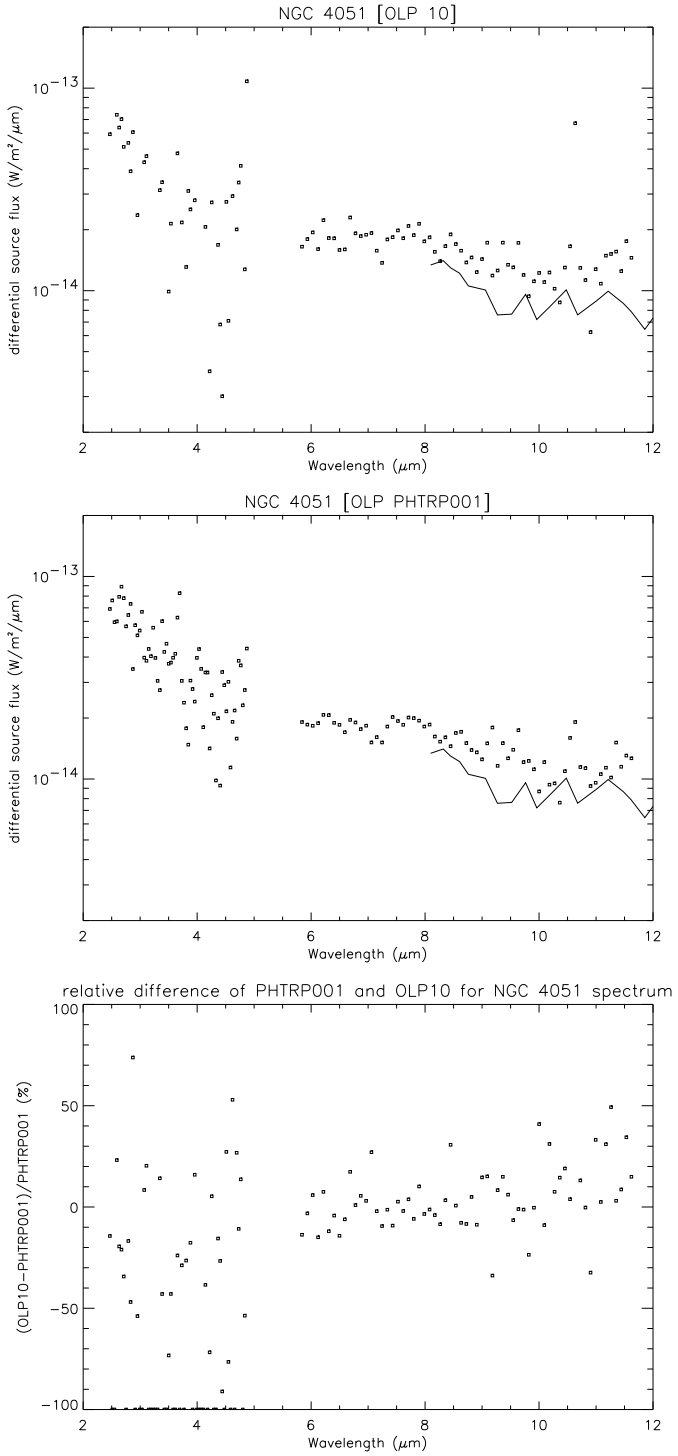

Figure 18: Comparison of the spectrum of NGC 4051 obtained in rectangular chopped mode (dots) with groundbased 8 – 13 micron spectroscopy (solid line) by Roche et al. 1991 for both OLP 10 (upper panel) and OLP PHTRP001 (middle panel) and the relative difference of both versions (lower panel).

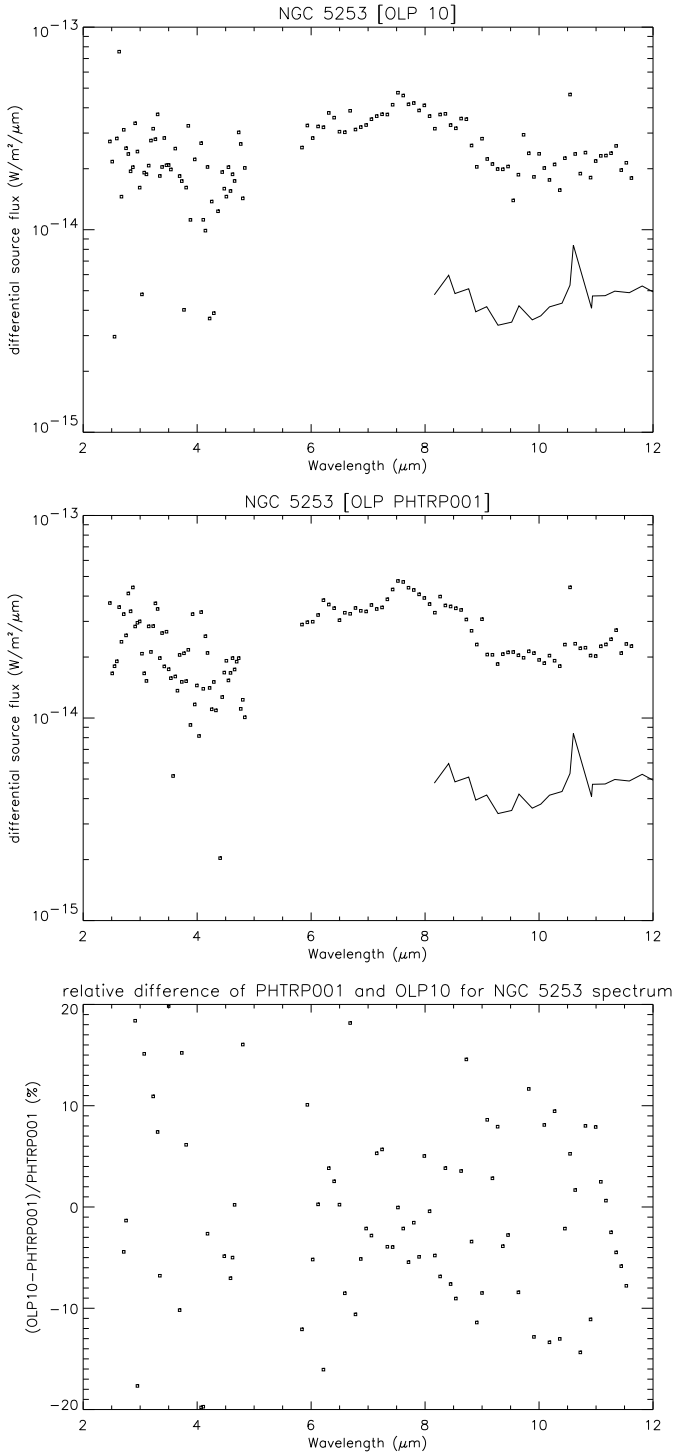

Figure 19: Comparison of the spectrum of NGC 5253 obtained in rectangular chopped mode (dots) with groundbased 8 – 13 micron spectroscopy (solid line) by Aitken et al. 1982 for both OLP 10 (upper panel) and OLP PHTRP001 (middle panel) and the relative difference of both versions (lower panel).

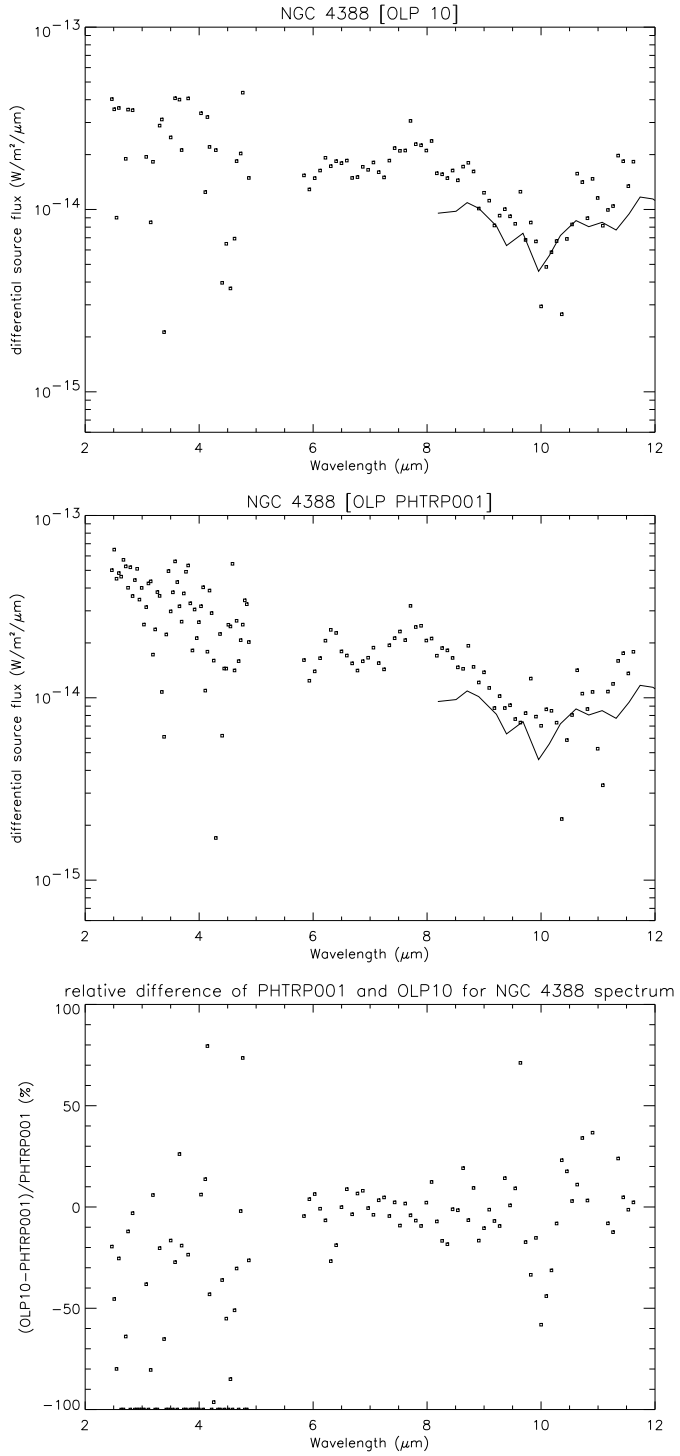

Figure 20: Comparison of the spectrum of NGC 4388 obtained in rectangular chopped mode (dots) with groundbased 8 – 13 micron spectroscopy (solid line) by Roche et al. 1991 for both OLP 10 (upper panel) and OLP PHTRP001 (middle panel) and the relative difference of both versions (lower panel).

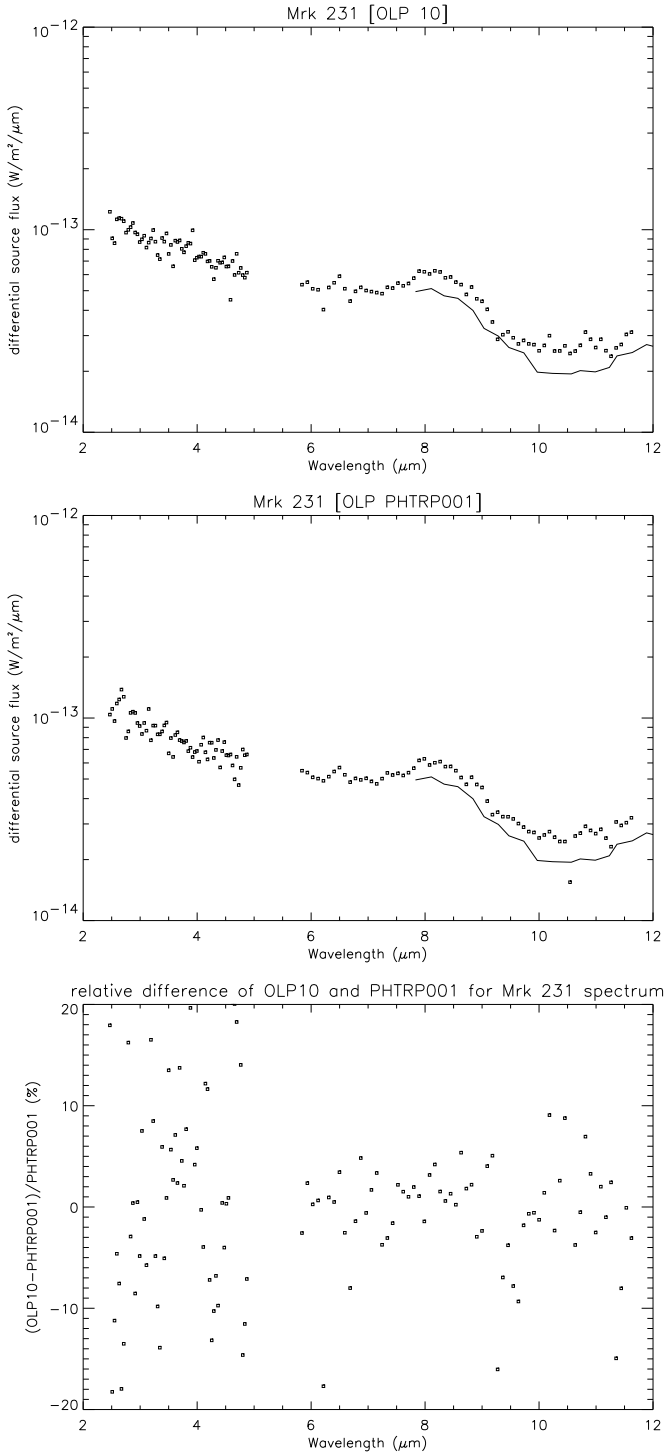

Figure 21: Comparison of the spectrum of Mrk 231 obtained in rectangular chopped mode (dots) with groundbased 8 – 13 micron spectroscopy (solid line) by Roche et al. 1991 for both OLP 10 (upper panel) and OLP PHTRP001 (middle panel) and the relative difference of both versions (lower panel).

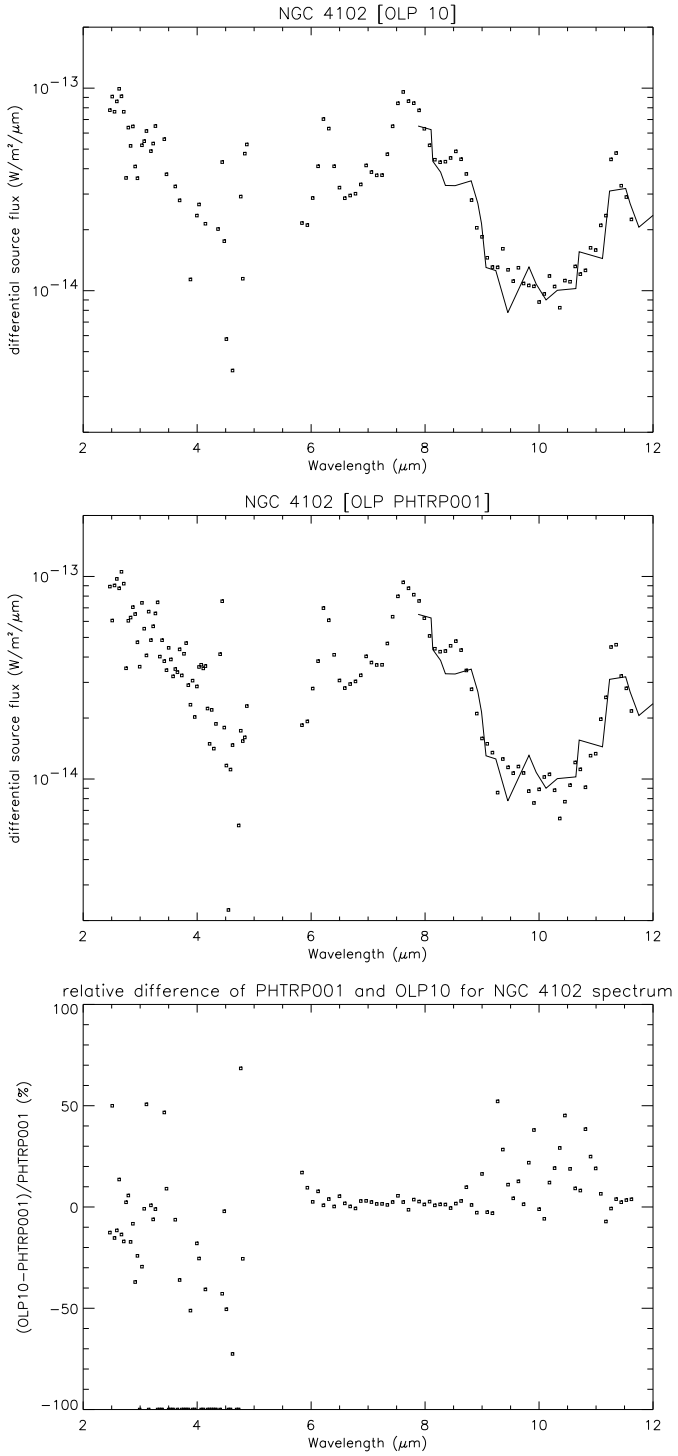

Figure 22: Comparison of the spectrum of NGC 4102 obtained in triangular chopped mode (dots) with groundbased 8 – 13 micron spectroscopy (solid line) by Roche et al. 1991 for both OLP 10 (upper panel) and OLP PHTRP001 (middle panel) and the relative difference of both versions (lower panel).

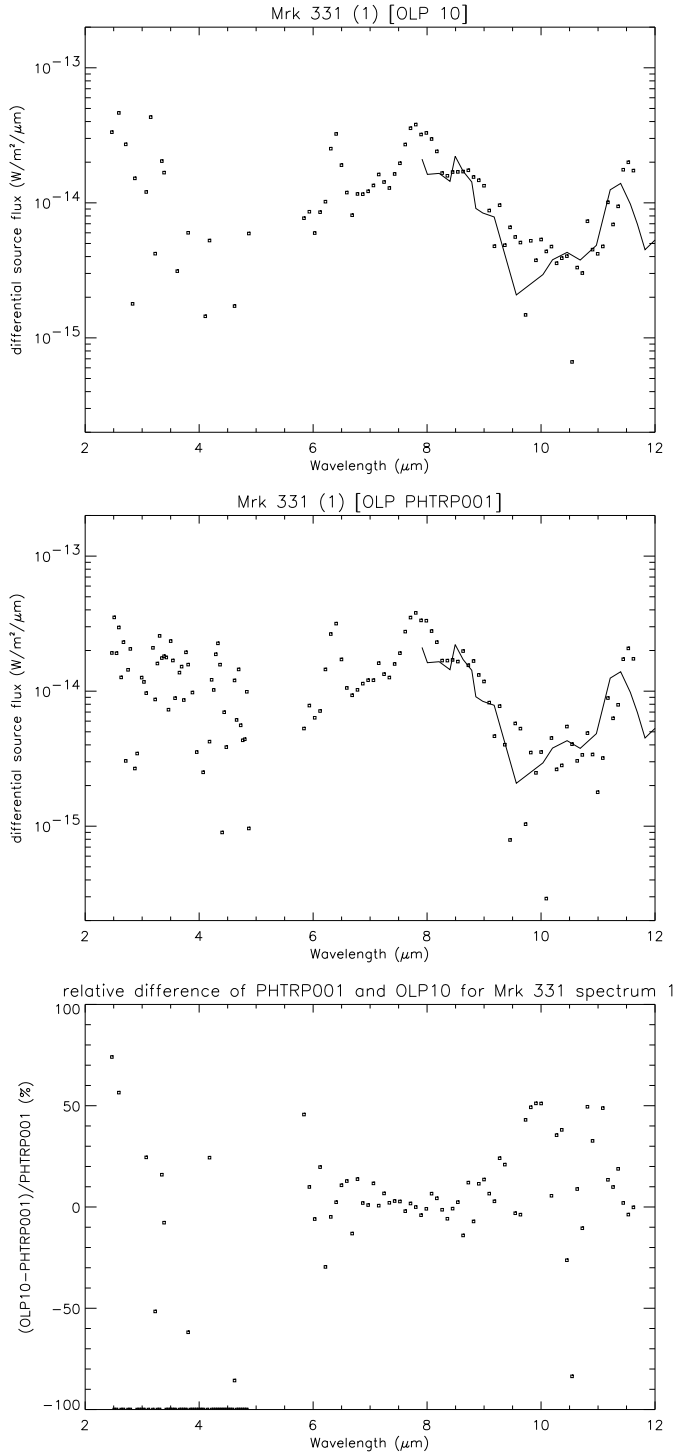

Figure 23: Comparison of the spectrum of Mrk 331 (1 = TDT37901644) obtained in triangular chopped mode (dots) with groundbased 8 – 13 micron spectroscopy (solid line) by Roche et al. 1991 for both OLP 10 (upper panel) and OLP PHTRP001 (middle panel) and the relative difference of both versions (lower panel).

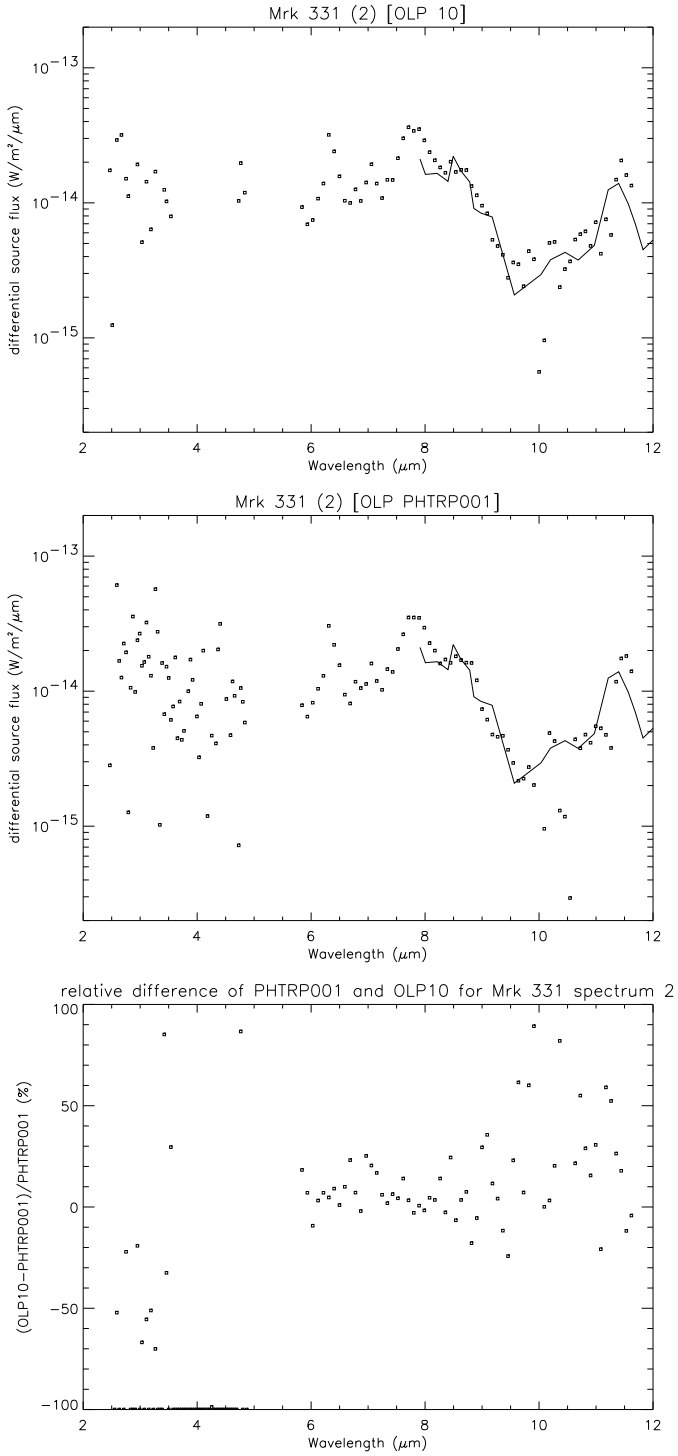

Figure 24: Comparison of the spectrum of Mrk 331 (2 = TDT56500644) obtained in triangular chopped mode (dots) with groundbased 8 – 13 micron spectroscopy (solid line) by Roche et al. 1991 for both OLP 10 (upper panel) and OLP PHTRP001 (middle panel) and the relative difference of both versions (lower panel).

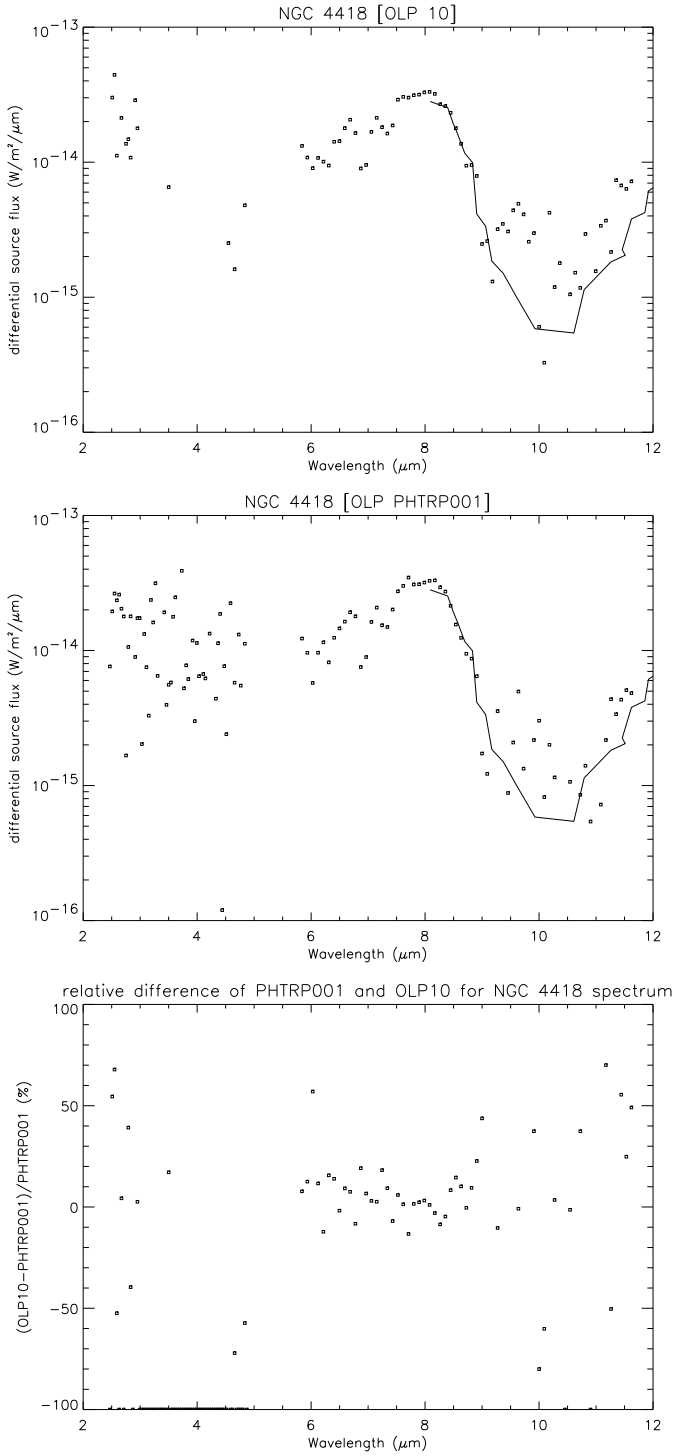

Figure 25: Comparison of the spectrum of NGC 4418 obtained in triangular chopped mode (dots) with groundbased 8 – 13 micron spectroscopy (solid line) by Roche et al. 1991 for both OLP 10 (upper panel) and OLP PHTRP001 (middle panel) and the relative difference of both versions (lower panel).

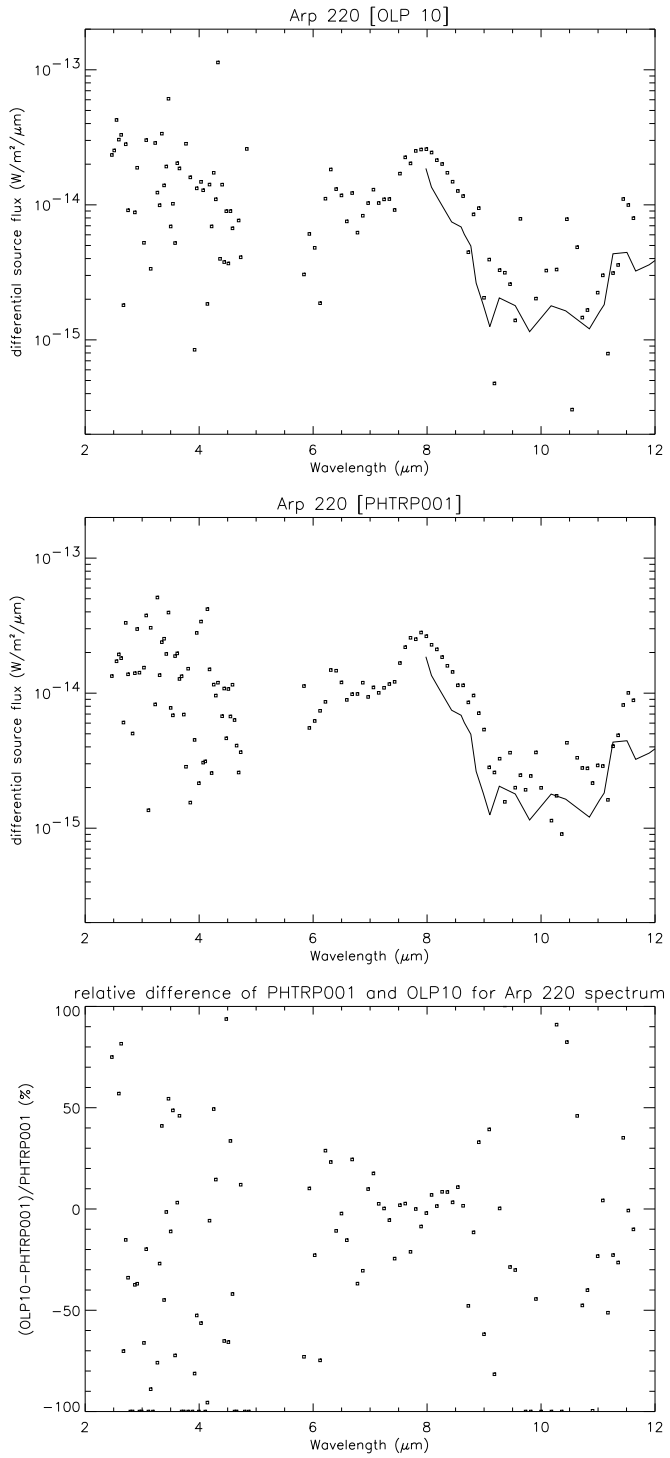

Figure 26: Comparison of the spectrum of Arp 220 obtained in rectangular chopped mode (dots) with groundbased 8 – 13 micron spectroscopy (solid line) by Roche et al. 1991 for both OLP 10 (upper panel) and OLP PHTRP001 (middle panel) and the relative difference of both versions (lower panel).

8 Summary and Conclusions

- The chopped mode spectroscopy has been successfully revalidated for OLP PHTRP001.
- For the measurements of standard stars, the absolute accuracy is better than ±10% for the flux range 2-15 Jy with the SS-array and 0.4-4 Jy with the SL-array (being ±5% over most of the range).
- The is excellent agreement between spectra obtained in rectangular and triangular chopped mode.
- The PHTRP001 spectra show very good agreement with groundbased 8 - 13 micron spectroscopy and the SL-continua are much smoother than for OLP 10 showing many more detections of PAH and atomic line features.

References

[1] U. Klaas and P. Richards, "Report on the PHT Scientific Validation for OLP Version 10.0", Version 1.0, 9-April-2002.

[2] R.J. Laureijs, U. Klaas, P.J. Richards, B. Schulz and P. Ábrahám, "The ISO Handbook, Volume V: PHT – The Imaging Photo-Polarimeter", SAI/99-069/Dc, Version 1.2, 01-July-2001

[3] P.L. Hammersley, M. Jourdain De Muizon, M.F. Kessler, P. Bouchet, R.D. Joseph, H. Habing, A. Salama, L. Metcalfe, "Infrared standards for ISO. I. A new calibration of mid infrared photometry", A&AS 128, 207, 1998

[4] J. Acosta, "Dynamic Calibration for ISOPHOT-S", IAC / IDC PHT internal calibration report, 03-August-1999

[5] P.F. Roche, D.K. Aitken, C.H. Smith and M.J. Ward, "An Atlas of Mid-infrared Spectra of Galaxy Nuclei", MNRAS 248, 606, 1991

[6] P.F. Roche, D.A. Allen, D.K. Aitken, "Symbiotic stars: spectrophotometry at 3-4 and 8-13 um", MNRAS 204, 1009, 1983

[7] C.H. Smith, D.K. Aitken, P.F. Roche, C.M. Wright, "Mid-infrared spectroscopy of galactic novae", MNRAS 277, 259, 1995

[8] N. Ginestet, J.M. Carquillat, C. Jaschek, "Spectral classifications in the near infrared of stars with composite spectra", 1999, A&A Supp 134, 473

[9] C.K. Mitrou, J.G. Doyle, M. Mathioudakis, E. Antonopoulou, "The emission of the RS CVn binaries in the IRAS passbands", 1996, A&A Supp 115, 61

[10] C.L. Perry, E.H. Olsen, D.L. Crawford, "A catalog of bright uvbybeta standard stars", 1987, PASP 99, 1184